

Microwave Spectroscopy of Deuterated Molecular Ions
and
Structures of Pyramidal XY_3 Molecules

MITSUNORI ARAKI
DOCTOR OF PHILOSOPY

Department of Structural Molecular Science
School of Mathematical and Physical Science
The Graduate University for Advanced Studies

1998

Acknowledgment

I wish to express my sincere gratitude to Professor Shuji Saito for his helpful guidance, valuable suggestions and kind encouragement throughout the course of this study. I am also grateful to Dr. Hiroyuki Ozeki for his kind helps and valuable advice during this study.

I am grateful to Professor Kojiro Takagi and Dr. Hitoshi Odashima of Toyama University and Dr. Hideo Fujiwara of the Institute for Molecular Science for their useful advice and helpful discussion.

I wish to thank Drs. Kei-ichi Namiki, Tsuyoshi Hirao, Inada Naomi, Kaori Kobayashi, Imtiaz K. Ahmad, Jian Tang and all the members in Department of Molecular Structure of the Institute for Molecular Science for their many helps, discussion and advice in my study and life.

I would like to express my gratitude to Professor Katsumi Kimura and Dr. Shin-ichiro Sato for their valuable and continued encouragement. Finally, I wish to express my special thanks to my parents for their continuous help and understanding.

Contents

1. INTRODUCTION	1
1.1 MICROWAVE SPECTROSCOPY OF MOLECULAR IONS	1
1.2 MOLECULAR IONS IN INTERSTELLAR CHEMISTRY	1
1.3 DEUTERATED MOLECULAR SPECIES IN INTERSTELLAR CHEMISTRY	3
1.4 POTENTIAL AND MOLECULAR STRUCTURE OF PYRAMIDAL XY_3 MOLECULES	6
REFERENCES	11
2. EXPERIMENTAL METHODS	15
2.1 PRODUCTION OF MOLECULAR IONS	15
<i>2.1.1 Hollow-cathode discharge</i>	<i>15</i>
<i>2.1.2 Magnetically confined DC-glow discharge</i>	<i>16</i>
2.2 EXPERIMENTAL APPARATUS	17
REFERENCES	20
3. MICROWAVE SPECTRUM OF THE INVERSION-ROTATION TRANSITIONS OF D_3O^+	24
3.1 INTRODUCTION	24
3.2 EXPERIMENTAL	26
3.3 MOLECULAR CONSTANTS, STRUCTURES AND INVERSION POTENTIAL	28
<i>3.3.1 Determination of molecular constants</i>	<i>28</i>
<i>3.3.2 Molecular structure of H_3O^+ and D_3O^+</i>	<i>32</i>
<i>3.3.3 $\Delta K = 3$ forbidden transitions</i>	<i>34</i>
<i>3.3.4 Rotational constants of H_2DO^+</i>	<i>35</i>
APPENDIX I	37
APPENDIX II	38
REFERENCES	39
4. MICROWAVE SPECTRUM OF THE SD_3^+ ION: MOLECULAR STRUCTURE	54
4.1 INTRODUCTION	54
4.2 EXPERIMENTAL	54
<i>4.2.1 Ion-drift Doppler shift correction</i>	<i>56</i>
4.3 MOLECULAR STRUCTURE	56
<i>4.3.1 r_z structure</i>	<i>57</i>
<i>4.3.2 r_e structure</i>	<i>58</i>
REFERENCES	59

5. MICROWAVE SPECTRA OF THE PURE ROTATIONAL TRANSITIONS OF HCNH⁺ AND ITS ISOTOPIC SPECIES	65
5.1 INTRODUCTION	65
5.2 EXPERIMENTAL	67
5.3 REST FREQUENCIES FOR ASTRONOMICAL SEARCHES	69
REFERENCES	73
6. SUMMARY	78

1. Introduction

1.1 Microwave spectroscopy of molecular ions

In recent years gaseous molecular ions have attracted much attention in the fields of high-resolution spectroscopy, plasma physics, interstellar chemistry and aeronomy. However, a limited number of simple molecular ions have been subjected to microwave spectroscopic studies which are essential to the characterization of precise molecular structure. This is because the positive charge of molecular cations generally gives large collisional cross sections with other molecules, making it difficult to produce a large amount of molecular ions required for microwave spectroscopy. Accordingly full characterization of even known simple molecular ions has rarely been presented from spectroscopic and molecular structural point of view.

1.2 Molecular ions in interstellar chemistry

Recent development of radio astronomy have thrown strong light on gaseous molecular ions which have turned out to be key molecules in the chemistry of various interstellar molecules detected by radio telescopes.

The first three interstellar molecules (CH , CH^+ and CN) were detected in diffuse clouds by ground-based optical telescopes around 1940. This is because generally dust grains in interstellar space present and attenuate transmission of visible light and observational spectroscopic studies in the optical region are limited to diffuse clouds. In contrast, radio wave propagates relatively freely through more dense molecular clouds in spite of large amount of dust grains. The first radio detection of interstellar molecule was made for the OH radical in 1963 [1] and an explosive growth in radio observations

followed from the detections of NH_3 [2], H_2CO [3] and H_2O [4] in 1968 - 69. In these 30 years one hundred molecular species have been detected in interstellar space by radio astronomical observations. It is generally accepted that the most abundant molecules in dark molecular clouds have been already detected and identified.

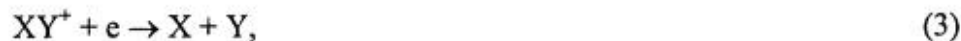
Production and destruction of interstellar molecules have been discussed from the early stage of their detections. Neutral-neutral reactions, endothermic reactions, and third body reactions have been generally used in the laboratory and chemical industry, but most of them are not efficient in the interstellar space of low temperature and low density. Instead of these chemical reactions, ion-molecule reaction was proposed to be efficient for production and destruction of molecules in space [5]. The reaction starts with cosmic-ray-induced ionization of H_2 and He , giving H_2^+ , H^+ and He^+ ions at first. And then the generated H_2^+ ion is converted into H_3^+ by a dissociative reaction with H_2 . The H_3^+ ion is extremely stable and a key molecular ion in interstellar chemical reactions. The ion reacts with neutral molecule and generates a more complicated ion, as given below:



HCO^+ and NH_2^+ ions are mainly produced from CO and N_2 , respectively, reacting with H_3^+ . Astronomical detection of HCO^+ and NH_2^+ strongly supports the ion-molecular reaction scheme. Furthermore, various ions are generated by a series of ion-molecular reactions as exemplified in the following formula



Finally the produced ions are converted into neutral molecules by dissociative recombination with electron,



H₂O and OH are generated, as given below



The ion-molecular reactions having no activation energy and showing no temperature dependence are efficient in the interstellar physical conditions of low temperature and low density, and the ions are extremely important intermediates in interstellar chemistry.

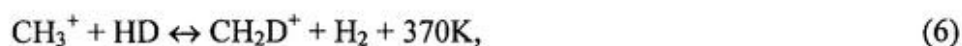
Since detections of the interstellar ions have been extremely limited, it is thought that any additional detection of interstellar ions may deepen understanding of interstellar chemistry. The detection of interstellar molecules is based on the astronomical observations of their spectral lines, whose rest frequencies are usually supplied from laboratory spectroscopy. Some of molecular ions were already studied by infrared spectroscopy for vibration-rotation transition. Calculated line frequencies from molecular constants determined by infrared spectroscopy are not sufficient in accuracy to detect and identify generally weak interstellar lines. Microwave spectroscopy is indispensable for supplying sufficiently precise transition frequencies required in astronomical observations. Accuracy of measured rotational transition frequencies is now improved to be several tens kHz and is suitable to astronomical observations. However, it is not easy to detect molecular ions even in the laboratory because of a difficulty in producing sufficient ions for microwave spectroscopy.

1.3 Deuterated molecular species in interstellar chemistry

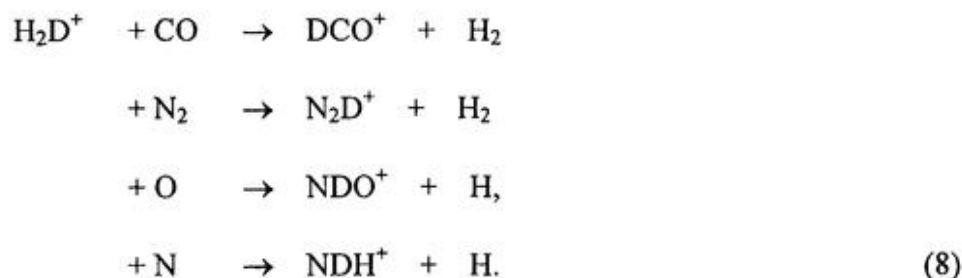
Several interstellar molecules have been found to have large D/H ratios enhanced by factors of $10^3 - 10^4$ over the primordial cosmic D/H ratio of $\sim 1.5 \times 10^{-5}$. For example,

the abundance ratio of $[\text{DCO}^+]/[\text{HCO}^+]$ is found to be 0.015 in Taurus Molecular Cloud 1 (dark cloud). This enhancement is called “deuterium enrichment.”

Fractionation of the deuterated species originates in exchange reactions of deuterium atom between molecules. Initially the deuterium atom exists in HD in dark molecular clouds. The deuterium enrichment in molecules occurs by the ion-molecular reactions including HD. Starting key interstellar reactions are as follows:



For reaction (5), ΔE is temperature-dependent, since the rate, k_r , of the reverse of (5) is $3.6 \times 10^{-18} \text{ cm}^3 \text{ s}^{-1}$ at 10 K and $2.0 \times 10^{-10} \text{ cm}^3 \text{ s}^{-1}$ at 70 K [6,7]. Owing to the lower value of ΔE for the reaction (5), it is effective only at lower temperatures (≤ 25 K), whereas reactions (6) and (7) become important at temperature up to ~ 100 K. The deuterium enhanced species, H_2D^+ , CH_2D^+ and C_2HD^+ , undertake subsequent reactions producing a variety of molecules of high deuterium concentrations [8]. H_2D^+ can participate in various reactions such as



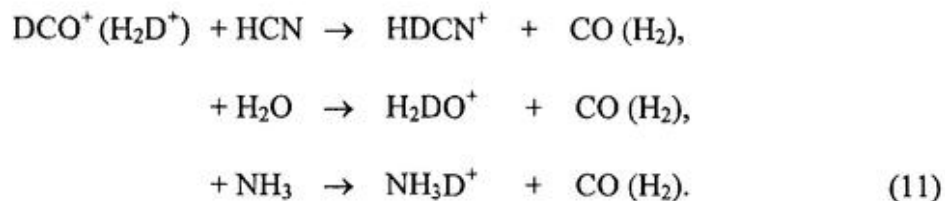
CH_2D^+ produced by the reaction (6) promotes several reactions, for example



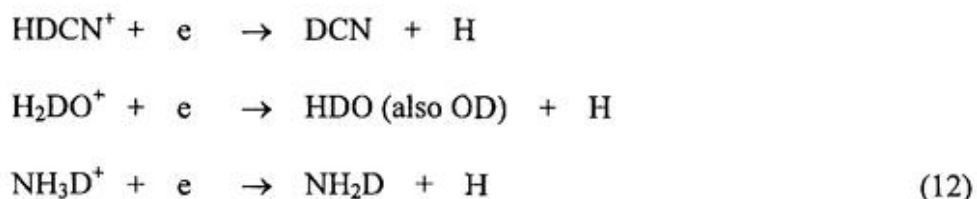
and



DCO^+ and H_2D^+ influences deuterium concentration of other molecules through reactions, as given below



Finally, dissociative recombination reactions with electrons give neutral deuterated species.



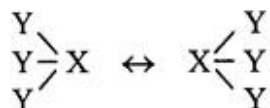
As can be seen from the above reactions, deuterated neutral molecules are generated in turn from the initial deuterated molecular ions H_2D^+ , CH_2D^+ and C_2HD^+ .

As discussed above, the degree of the deuterium enrichment is determined by physical conditions and the reactions involved in interstellar molecular clouds. Distribution of deuterium atoms in related molecules supplies information about these reactions. In other words the deuterium enrichment is generally a good probe to study the reaction scheme in space.

In order to determine the D/H ratio of molecule in the molecular clouds, spectral lines of the deuterated species must be observed using radio telescopes. A call for precise transition frequencies has promoted laboratory spectroscopy of important deuterated species.

1.4 Potential and molecular structure of pyramidal XY_3 molecules

The XY_3 type molecules are important in molecular spectroscopy and are classified into two types. One is planar XY_3 type such as CH_3^+ which has D_{3h} symmetry. The other is pyramidal XY_3 type which has C_{3v} symmetry and shows complicated but interesting features in spectroscopy. A molecule of the latter type has a double minimum potential, and quantum mechanically shows inversion motion in which the X atom moves through the Y_3 plane to take an identical but inverted pyramidal configuration, such as



The eigenfunctions of the molecule can be expressed as linear combinations of ϕ_L and ϕ_R wavefunctions corresponding to the equivalent right and left configurations, respectively.

The functions are described as

$$\psi_+ = \frac{1}{\sqrt{2}}(\phi_L + \phi_R)$$

and

$$\psi_- = \frac{1}{\sqrt{2}}(\phi_L - \phi_R), \quad (13)$$

which have opposite symmetry for inversion through a plane containing three Y atoms.

The pyramidal molecules having the double minimum potential are further classified into two groups. One group has a high inversion barrier in the double minimum potential, and SiH_3 , PH_3 and SH_3^+ belong to this group. Theoretically, all pyramidal XY_3 molecular species shown inversion motion, but, in fact, splitting due to the inversion motion is observable for only limited number of species. Inversion splittings of PH_3 and

SH_3^+ are extremely small due to the barrier height of 30.8 and 34.8 kcal/mol, respectively [9]. The inversion frequency of PH_3 is so small, less than 1 kHz, that high-resolution spectroscopy cannot resolve it. The other group has a large inversion splitting due to a low inversion barrier, as found in NH_3 . The inversion barrier of NH_3 is reported to be 5.74 kcal/mol [10]. The inversion potential curve of NH_3 is described in figure 1.1. The potential energy of the molecule is plotted as a function of the distance between the N atom and H_3 plane and has double minima corresponding to the two equivalent equilibrium configurations.

Before the observation of the inversion splitting of NH_3 , models of the double minimum potential were proposed. In 1932, Dennison and Uhlenbeck suggested a potential which consisted of two equal parabolas connected by a straight line [11]. However, the assumed potential was somewhat artificial. Manning developed another potential in 1935 [12], such as

$$V(r) = -C \operatorname{sech}^2 r/2\rho + D \operatorname{sech}^4 r/2\rho \quad (14)$$

where r is the distance from the N atom to the H_3 plane and C , D and ρ are constants. The constant ρ is proportional to $\mu^{1/2}$, where $\mu = 3mM/(3m + M)$, m is the mass of hydrogen atom and M the mass of nitrogen atom. This formula was found to predict vibrational frequencies well. It enabled, through the dependence on μ , the prediction of the isotopic shifts of the inversion frequency. In 1933, Cleeton and Williams observed the inversion of NH_3 for the first time as a broad absorption band at atmospheric pressure in the region of 1 cm wave-length [13]. After several spectroscopic studies of NH_3 [14], in 1962 Weeks *et al.* presented a potential composed of a double minimum and a system of harmonic oscillators for the remaining four vibrational modes [15]. In 1973, Papoušek *et al.* described a new

model to study the vibration-inversion-rotation energy levels of NH_3 [16]. In this model the inversion motion is removed from the vibration problem and considered with a rotational problem by allowing the molecular reference configuration to be a function of the large amplitude motion coordinate. Recently, most high resolution spectroscopic data of NH_3 and its isotopic species were analyzed with this model.

Relation of the inversion splitting to the double minimum potential is indicated as follows [11]

$$\nu_0 = \nu \left(\frac{1}{\pi A^2} \right) \quad (15)$$

where

$$A = \exp \left\{ \frac{2\pi}{\hbar} \int_0^r [2\mu(V(r) - E_0)]^{1/2} dr \right\}$$

and

- ν_0 : inversion splitting
- ν : the fundamental vibrational frequency
- $V(r)$: the double minimum potential function
- E_0 : the energy level in the vibrational ground state
- r_1 : bond length at $V = E_0$.

The equation (15) shows that the inversion splitting does not depend upon the form of the curve but only upon a square root area

$$\frac{2\pi}{\hbar} \int_0^r [2\mu(V(r) - E_0)]^{1/2} dr \quad (16)$$

in the non-classical region. The area of the double minimum potential are illustrated in figure 1.2. The equation (15) indicates that the inversion splitting is one of the most important information in order to determine the double minimum potential.

Since effective tunneling occurs only when the barrier of double minimum potential

is low and narrow, it is essential to examine a molecule of low and narrow barrier showing the barrier tunneling of pyramidal XY_3 type molecules. The inversion barrier of H_3O^+ was reported to be 2.03 kcal/mol [17] and its potential is illustrated in figure 1.1. Its barrier height is about one-third of that of NH_3 , and the width is much narrower than that of NH_3 . Observation of H_3O^+ and its deuterium species D_3O^+ can provide detailed information for the barrier tunneling and the double minimum potential. In this study, we have observed the inversion-rotational transition of D_3O^+ for the first time by microwave spectroscopy and determined its inversion splitting in the ground vibrational state to be $15.35550086(147) \text{ cm}^{-1}$, where the number in parentheses denotes one standard error. Furthermore, the inversion splitting in the $\nu_2 = 1$ inversion mode was determined from our results to be $191.38874(98) \text{ cm}^{-1}$ in combination with the infrared data of the $\nu_2(1^+ - 0^+)$ and $\nu_2(1^+ - 0^-)$ transitions studied by Petek *et al.* [18]. The two precise inversion splittings are useful to improve the double minimum potential of H_3O^+ .

Molecular structure is the most fundamental property to characterize a molecule, and the following several kinds of molecular structure have been proposed. The well-known r_0 structure is derived from the rotational constant B_0 of the molecule in the ground state, but it suffers from the effect of zero-point vibrations and is obscure in a physical viewpoint. The zero-point average structure (r_z structure), which corresponds to the average positions of nuclei in the ground state, can be determined by taking into account the harmonic zero-point corrections to the rotational constants. The equilibrium structure (r_e structure), defined at the bottom of the potential surface, is most physically meaningful (see figure 3.4). The r_e structure is calculated from the equilibrium rotational constants B_e which are obtained from B_0 by correcting changes of the rotational constants B_v due to the

excitation of each fundamental mode. The pyramidal XY_3 type molecule has six fundamental vibrational modes, two of which are doubly degenerate. Therefore, one must determine the rotational constants for at least four different vibrational states. However, transition dipole moments which determine intensities of vibrational transitions depend more strongly on the vibrational mode. For example, infrared intensities of H_3O^+ was reported to be 36.5, 504.3, 1107.5 and 232.4 $km\ mol^{-1}$ in the ν_1 , ν_2 , ν_3 and ν_4 modes, respectively [19]. The ν_2 and ν_3 modes were already observed (see chapter 3), but not the ν_1 and ν_4 modes. Thus, the r_e structure of H_3O^+ can not be easily obtained by the above orthodox method. However, it was shown in this study that the r_e structure of H_3O^+ and H_3S^+ can be derived with a diatomic approximation to the bond.

References

- [1] WEINREB, S. BARRETT, A. H., MEEKS, M. L., and HENRY, J. C., 1963, *Nature (Lond.)*, **200**, 829.
- [2] CHEUNG, A. C., RANK, D. M., TOWNES, C. H., THORNTON, D. D., and WELCH, W. J., 1968, *Phys. Rev. Lett.*, **21**, 1701.
- [3] SNYDER, L. E., BUHL, D., ZUCKERMAN, B., and PALMER, P., 1969, *Phys. Rev. Lett.* **22**, 679.
- [4] CHEUNG, A. C., RANK, D. M., TOWNES, C. H., THORNTON, D. D., and WELCH, W. J., 1969, *Nature (Lond.)*, **211**, 626.
- [5] HERBST, E., and KLEMPERER, W., 1973, *Astrophysical J* , **185**, 505.
- [6] HERBST, E., 1982, *Astron. Astrophys.*, **111**, 76.
- [7] SMITH, D., ADAMS, N. G., and ALGE, E., 1982, *Astrophys. J.*, **263**, 123.
- [8] WATSON, W. D., 1976, *Rev. Mod. Phys.*, **48**, 513.
- [9] YAMABE, T., AOYAGI, T., NAGATA, S., SAKAI, H., and FUKUI, K., 1974, *Chem. Phys. Lett.*, **28**, 182.
- [10] ŠPIRKO, V., 1983, *J. molec. Spectrosc.*, **101**, 30.
- [11] DENNISON, D. M. and UHLENBECK, G. E., 1932, *Phys. Rev.*, **41**, 313.
- [12] MANNING, M. F., 1935, *J. chem. Phys.*, **3**, 136.
- [13] CLEETON, C. E. and WILLIAMS, N. H., 1934, *Phys. Rev.*, **45**, 234.
- [14] for example: BENEDICT, W. S. and PLYLER, E. K., 1957, *Can. J. Phys.*, **35**, 1235.
- [15] WEEKS, W. T., HECHT, K. T., and DENNISON, D. M., 1962, *J. molec. Spectrosc.*, **8**, 30.

- [16] PAPOUŠEK, D., STONE, J. M. R., and ŠPIRKO, V., 1973, *J. molec. Spectrosc.*, **48**, 17.
- [17] ŠPIRKO, V., and KRAEMER, W. P., 1989, *J. molec. Spectrosc.*, **134**, 72.
- [18] PETEK, H., NESBITT, D. J., OWRUTSKY, J. C., GUDEMAN, C. S., YANG, X., HARRIS, D. O., MOORE, C. B., and SAYKALLY, R. J., 1990, *J. chem. Phys.*, **92**, 3257.
- [19] SWANTON, D. J., BACSKAY, G. B., and HOSH, N. S., 1986, *Chem. Phys.*, **107**, 9.

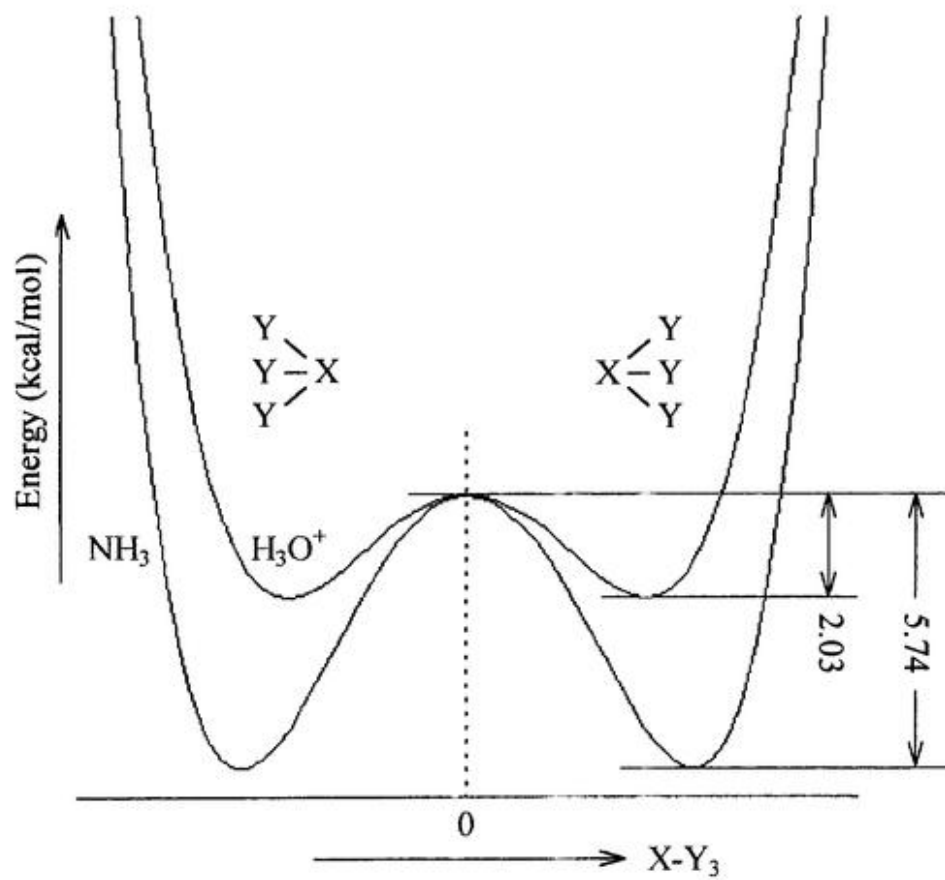


Figure 1.1 The double minimum potential of NH_3 and H_3O^+ .

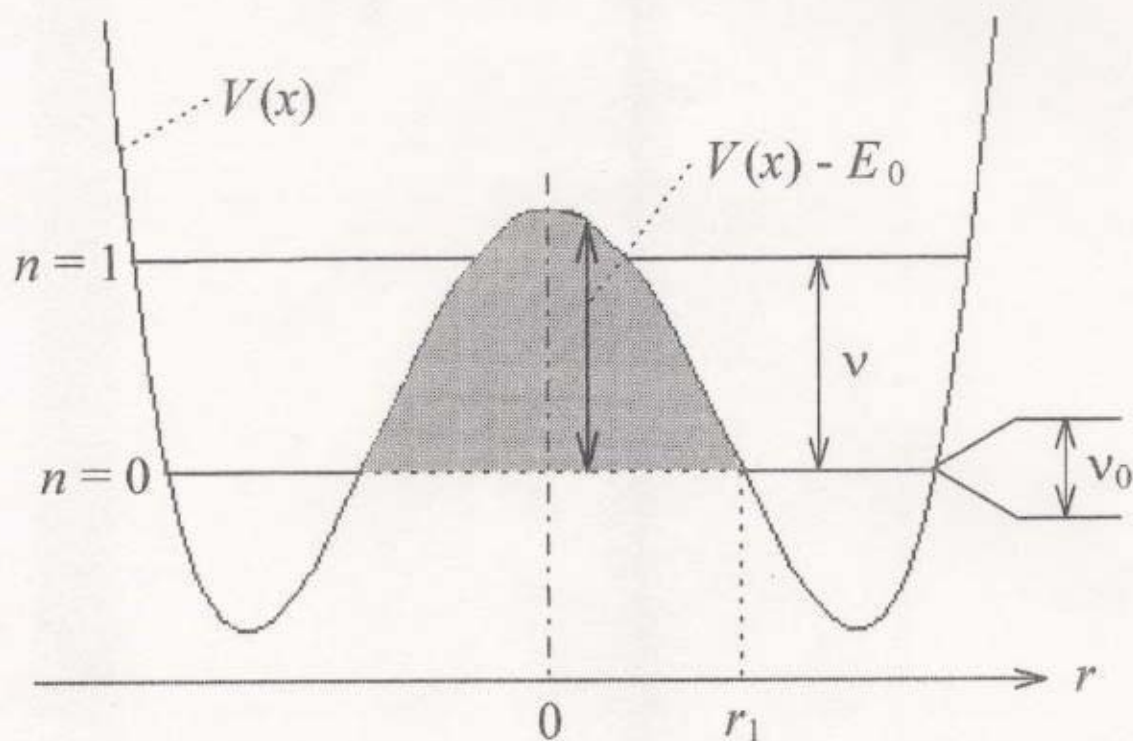



Figure 1.2 Relation of several signs to the double minimum potential of the pyramidal XY_3 molecule. In this diagram, we assumed that the inversion splitting ν_0 is sufficiently small compared with the vibrational frequency ν . r is the pyramidal height, i.e. the distance from the X atom to the Y_3 plane. n is the vibrational quantum number. An area indicated by equation (16) is shown with “”. Details of the other signs are given in the text.

2. Experimental Methods

2.1 Production of molecular ions

Molecular ions rapidly react with environmental molecules and materials due to its large collisional cross section, and it is very difficult to generate a large amount of the ions sufficient for detection of the rotational spectral lines with microwave spectroscopy. Therefore, a good production method in the absorption cell is very important for microwave spectroscopy of molecular ions. We have examined two effective ion production methods, hollow-cathode discharge and magnetically confined DC-glow discharge.

2.1.1 Hollow-cathode discharge

The present absorption cell is a free space cell with 2 m length and 10 cm diameter, and is cooled by circulating liquid nitrogen through a copper tube soldered on a copper sheet covering the glass cell. A sample gas mixture is introduced into the cell through a side tube on the anode side, and the discharged mixture is pumped out from the cell through another side tube on the cathode side with an oil diffusion pump. Two short cylindrical electrodes, about 20 cm length, in the cell were used to produce various free radicals by a DC-glow discharge directly in the cell. However, the method is not satisfactorily suitable for production of the ions.

Several molecular ions were studied with microwave spectroscopy using hollow-cathode discharge technique [1]. We employed the hollow cathode to produce sufficient amount of ions in the cell [2]. The configuration of the hollow-cathode discharge is illustrated in figure 2.1(a). Hollow-cathode effect shows three characteristics: (i) electrons

in discharge vertically jump out of the inner surface of the cathode in strong acceleration, (ii) current density in the cathode increases, and (iii) high and low energy electrons increase due to distribution of electron energy. As a result, abundant ions are produced in the discharge cell. So as to achieve the high current density in a cell, a small diameter cell is more advantageous than a large diameter one. In infrared spectroscopy, many species of ions were observed with the small diameter discharge cell [1]. This is not applicable to microwave spectroscopy because the small diameter cell is known to disturb propagation of microwave having a larger wavelength. Therefore, the 10 cm diameter cell was employed in the present study. We found that the hollow-cathode discharge is very efficient in producing several molecular ions. The D_3O^+ and D_3S^+ ions were studied with this method.

2.1.2 Magnetically confined DC-glow discharge

The method of magnetically confined DC-glow discharge was developed by De Lucia *et al.* as a technique for enhancement of positive-ion concentrations [3]. The enhancement in the ion signal strength, as measured by microwave spectroscopy, was 18 - 20 times in HCO^+ and NH_2^+ when a 200 G magnetic field was applied to the discharge cell. The magnetic field effect on H_3^+ and DCO^+ was also investigated using infrared spectroscopy [4]. Bogey *et al.* reported an observation of H_3O^+ in the submillimeter-wave region using the enhancement with magnetic field [5]. In the magnetically confined DC-glow discharge, the enhancement of positive ion occurs due to a lengthening of the ion-rich negative glow as well as an additional enhancement caused by increased density of ionizing electrons, as shown in figure 2.1(b). The method is employed for efficient

production of protonated ions in the absorption cell.

We have examined the method with our microwave spectrometer. Around the absorption cell was wound a solenoid of enameled wire to generate the magnetic field, and two short electrodes, about 10 cm length, were employed. We studied the hydronium ion H_3O^+ and measured intensity of the $J = 3^+ \leftarrow 2^-$, $K = 2$ transition at 364.8 GHz. The ion was generated by a gas mixture of H_2O , H_2 and He. The magnetic field was applied to the cell up to 130 G. The normalized signal intensity of the H_3O^+ ion was plotted against the applied magnetic field and is shown in figure 2.2. The intensity increased in proportion to the magnetic field up to 50 G and reached a maximum at 70 - 80 G with our spectrometer. It was concluded that the method of a magnetically confined DC-glow discharge is extremely effective to produce the protonated ion in the present microwave spectrometer. We measured the HCNH^+ ion and its isotopic species, which could be observed only by this method.

2.2 Experimental apparatus

A source-modulated microwave spectrometer at the Institute for Molecular Science was used in the present study [6,7]. The block diagram of the spectrometer is shown in figure 2.3. This spectrometer is mainly composed of a radiation source, microwave circuits, frequency standard, an absorption cell, a detector, amplifiers, and electronic circuits.

As radiation sources, several millimeter-wave klystrons were used in the region between 55 and 155 GHz, while the output from frequency multipliers (doubler, tripler and quadrupler) was applied in the region above 120 GHz. By a combination of the multipliers the upper limit of the covered region reach to the frequency of 620 GHz. The

source radiation of the klystrons was modulated by a bi-directional square wave of 50kHz. The output radiation from the multiplier was collimated by a rectangular horn and a teflon lens, and traveled through the free-space absorption cell. The radiation was focused on a liquid-He cooled indium-antimonide (InSb) detector with a second teflon lens. The detector output was amplified by a preamplifier and then lock-in amplified by a phase sensitive detector (PSD) in the $2f$ (100 kHz) mode. The signal was recorded to a personal computer as a second-derivative waveform in the frequency. On the other hand, the microwave frequency of the klystron source was measured by comparison with a frequency standard (8 - 12 GHz) of a centimeter-wave YIG oscillator, and was scanned over a few MHz range by a saw-tooth voltage applied to the reflector of the source klystron with a repetition rate of about 5 Hz. The frequency of the YIG oscillator was directly measured by a frequency counter, and interfaced to the personal computer.

So as to detect the molecular ions, not only the sufficient production but also sensitivity of the spectrometer is indispensable. Intensity of the rotational spectral line is proportional to a square of permanent dipole moment of a molecule and a square or a cube (linear molecule) of the transition frequency. Thus the intensity of rotational lines increases in a high frequency region. The present microwave spectrometer can be used up to a frequency of 620 GHz, and the radiation sources can produce high power output up to 400 GHz. The spectrometer is advantageous for sensitive detection of molecules because of the covered frequency region.

$^{18}\text{O}^{13}\text{C}^{34}\text{S}$ is an isotopic species of carbonyl sulfide and has a natural abundance of 0.93 ppm and a permanent dipole moment of 0.72 D. The typical sensitivity of the spectrometer was examined at 277 GHz by observing the $J = 25 - 24$ transition of this

molecule [8]. A signal-to-noise ratio was about 20 by integration for 20 s. The minimum detectable peak absorption coefficient by integration for 200 s was estimated to be $7.5 \times 10^{-10} \text{ cm}^{-1}$. In the present 2 m free space cell, the coefficient corresponds to the minimum detectable total number of molecules of 10^{11} , or the minimum detectable density of 10^7 molecules/cm³. This high sensitivity is a result of the combination of low noise and high power source, a low noise detector, and a highly conductive cell in the microwave region, and is essential to detect the molecular ions.

References

- [1] for example: LIU, D. -J., HAESE, N. N., and OKA, T., 1985, *J. chem. Phys.*, **82**, 5368;
HO, W. C., PURSELL, C. J., and OKA, T., 1991, *J. molec. Spectrosc.*, **149**, 530.
- [2] THE ELECTRIC SOCIETY, 1975, *Discharge Handbook* (Ohm).
- [3] DE LUCIA, F. C., HERBST, E., PLUMMER, G. M., and BLAKE, G. A. 1983, *J. chem. Phys.*, **78**, 2312.
- [4] K. KAWAGUCHI, C. YAMADA, S. SAITO, and E. HIROTA, 1985, *J. chem. Phys.* **82**, 1750.
- [5] BOGEY, M., DEMUYNCK, C., DEMIS, M., and DESTOMBES, J. L., 1985, *Astron. Astrophys.*, **148**, L11.
- [6] YAMAMOTO, S., and SAITO, S., 1988, *J. chem. Phys.*, **89**, 1936.
- [7] SAITO, S., and GOTO, M., 1993, *Astrophys. J.*, **410**, L53.
- [8] OZEKI, H., and SAITO, S., 1996, *Kotai-butsu i*, **31**, 343.

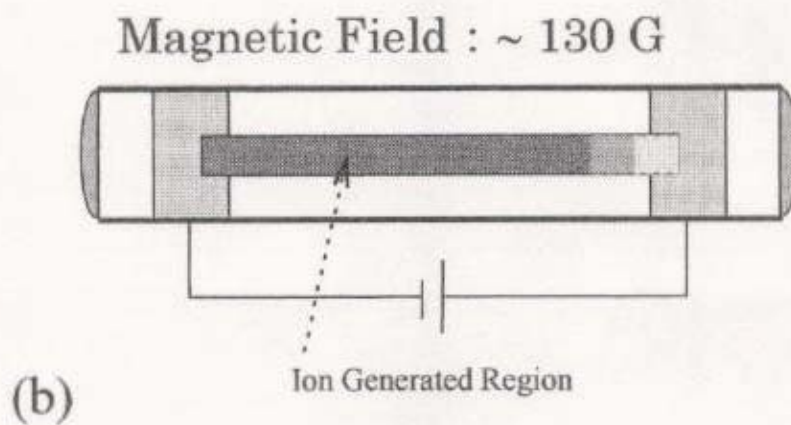
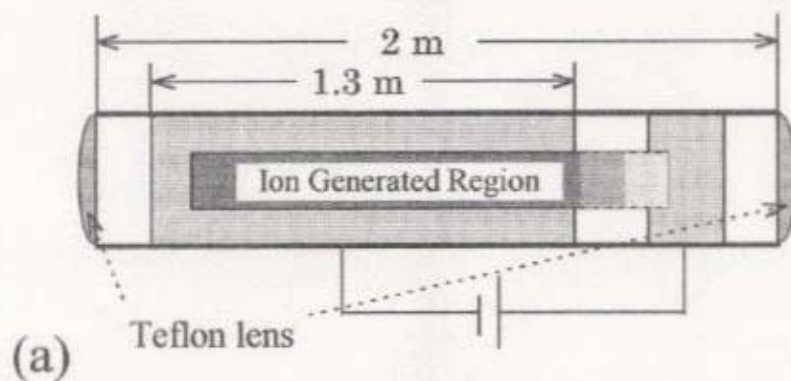


Figure 2.1. The hollow-cathode discharge (a) and the magnetically confined DC-glow discharge (b) in the absorption cell.

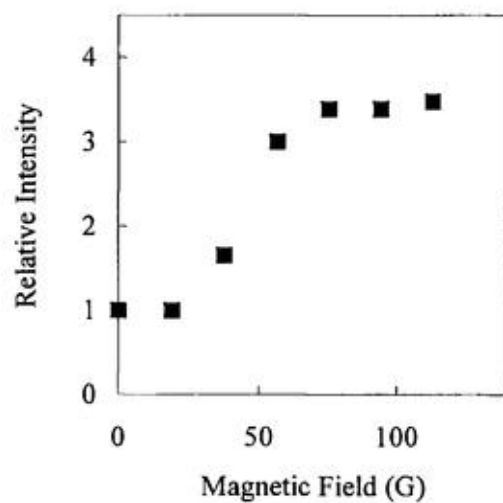


Figure 2.2. Approximate relation between the intensity of H_3O^+ and the magnetic field.

The intensity at 0 G is taken to be 1.0.

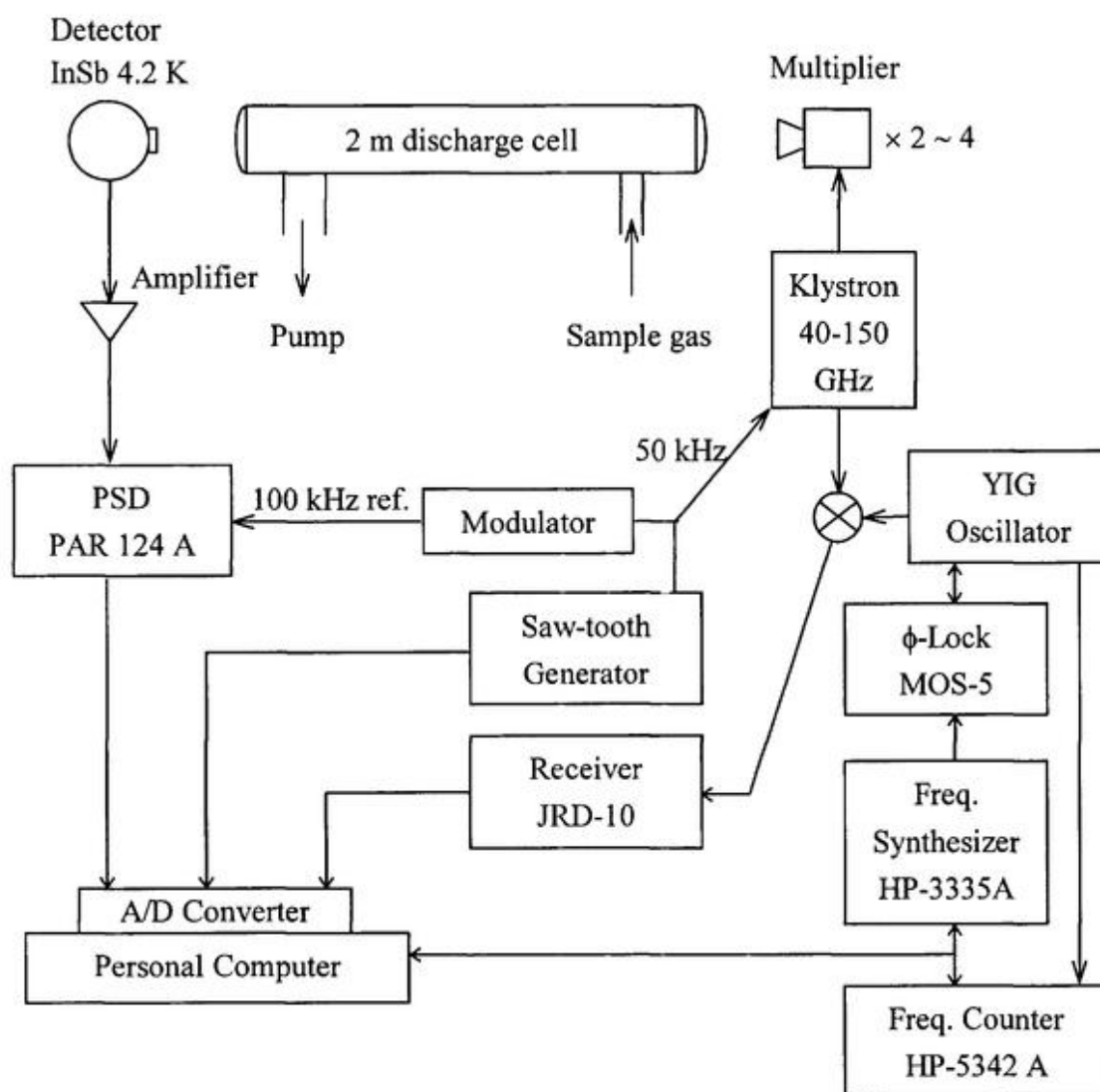


Figure 2.3. Block diagram of the source-modulated microwave spectrometer at the Institute for Molecular Science.

3. Microwave Spectrum of the Inversion-Rotation Transitions of D_3O^+

[*Journal of Chemical physics*, **109**, 5707 (1998) *Communications*]

[*Molecular physics*, accepted]

3.1 Introduction

The hydronium ion, H_3O^+ , is one of the most fundamental species in aqueous acid-base chemistry, and also in gas-phase interstellar chemistry. The ion is isoelectronic to ammonia showing an “umbrella inversion motion” and has been extensively studied spectroscopically. The first high-resolution spectroscopy of the gaseous H_3O^+ ion was carried out by Begemann *et al.* in 1983 [1,2] who reported the laser infrared study of the ν_3 band. Since then several experimental studies have been devoted to the ν_2 band, all of which focused on determining the tunneling splitting for the inversion motion [3-6]. However, a direct measurement of the tunneling doublet, which was essential to locating the lowest absolute energy levels of H_3O^+ , was not successful until 1985 [5,7]. Liu and Oka measured the crucial inversion separation in the $\nu_2 = 1$ state, $1^- - 1^+$, and derived the ground state splitting for the first time [5,7,8]. Soon after this study the separation was refined by direct observation with submillimeter-wave and far-infrared spectroscopy [9-12]. In the meantime, theoretical studies had been developed to predict the potential surface and the rotation-inversion-vibration energy levels of H_3O^+ [13-18].

In contrast to the normal species, spectroscopic studies of the fully deuterated species, D_3O^+ , are extremely limited. So far two infrared studies were reported on the vibration-rotation transition of ν_2 [19] and ν_3 [20], but the inversion splitting in the zeroth vibrational level was predicted only by using a nonrigid inverter model. The experimental determination of the splitting of D_3O^+ is as equally crucial as that of H_3O^+ [21]. We report

the first direct observation of the inversion splitting of the D_3O^+ ion by microwave spectroscopy.

The pyramidal XY_3 type molecule has two independent structural parameters, i.e. X–Y bond length (r) and X–Y–X bond angle (θ). Determination of both rotational constants B and C is essential for the precise characterization of the molecular structure, especially for prediction of spectral lines of H_2DO^+ , which is an important probe for deuterium fractionation of interstellar H_2O and OH. However the constant C cannot be obtained from normally allowed transitions, because the selection rule constrains the allowed transitions to those with the rotational quantum number K being unchanged. Molecules such as NH_3 and H_3O^+ , which show inversion splitting, have D_{3h} symmetry, and the $\Delta k = \pm 3n$ ($|k| = K$) interactions occur between levels of different inversion symmetry [12,22-25]. The interaction arises from the fourth-order contributions of the inversion-rotation interaction due to harmonic, Coriolis and anharmonic effects. Such interactions may allow us to determine C (in the second order) from the energy shifts without direct observation of forbidden transitions. In the case of H_3O^+ , the $(J^+, K = 0)$ energy level is close to the $(J, 3)$ level since the inversion splitting happens to be close to $9(C - B)$ in the 0^+ state. The $|\varphi(s); J, 0\rangle$ and $|\varphi(a); J, 3\rangle$ wavefunctions mix strongly, where s (or $+$) and a (or $-$) signs indicate lower and upper levels, respectively, in the inversion splitting, and the energy levels are significantly shifted. The interaction produces observable shifts of the levels in infrared spectroscopy. The rotational constant C and the interaction parameters of H_3O^+ were spectroscopically determined from the pure inversion transitions by Verhoeve *et al.* [12]. Uy *et al.* also reported the interaction parameters and the rotational constant C from the observation of forbidden $\Delta|k - l| = 3$ transitions in the ν_3

band [25].

For D_3O^+ , the energy differences between the $(J^+, 0)$ and $(J, 3)$ energy levels are larger than those of H_3O^+ , and the energy level shifts are small compared with those of H_3O^+ . However, the small shifts are detectable using microwave spectroscopy of sufficient high resolution. The interactions give the most conspicuous effect for the $K = 3$ levels. So as to determine the interaction parameters of D_3O^+ , a large number of lines including some $K = 3$ lines should be measured. In this study, we have measured precisely the $J = K \sim J = K + 5$ series lines of Q-branch and five P-branch transitions. The observed fifty three P- and Q-branch transitions and six combination differences from infrared data were included in the present analysis. The analysis of these data yields the $\Delta k = \pm 3n$ interactions parameters and the rotational constants C . We presented r_z structures of H_3O^+ and D_3O^+ , equilibrium structure of H_3O^+ and estimated rotational constants of H_2DO^+ , which are derived from the observed rotational constants.

3.2 Experimental

The inversion-rotation spectra of D_3O^+ were measured using the experimental apparatus described in chapter 2. The ion was generated in the free space absorption cell by the hollow-cathode discharge of a mixture of D_2O and D_2 gases. At first, intensity of a H_3O^+ line was monitored and its optimum conditions were deduced. These same conditions were used for the initial observation of the D_3O^+ ion. Spectral lines of the D_3O^+ ion were initially searched on the basis of the calculated inversion spectrum obtained from an analysis with a nonrigid inverter Hamiltonian by Sears *et al.* [19]. They predicted that the strong Q-branch transitions $J = K$ ($K = 1, 2, 3, \dots$) lie around 460 GHz. A stick diagram

of the predicted spectrum is shown in figure 3.1(a). We found a series of lines that appeared from 459.9 GHz and showed a relatively large line width and the same production behavior. Their signal intensities decreased to one half or one third when a magnetic field of several tens of gauss was also applied to the cell [26,27], as shown in figure 3.2. The same behavior was also observed for lines of H_3O^+ . The spectral lines were readily assigned to Q-branch transitions with $J = K$, for which a stick diagram of the observed spectrum is described in figure 3.1(b). These assignments enabled us to predict another series of Q-branch and P-branch transitions with high accuracy. So far we observed 5 P-branch and 48 Q-branch transitions in the frequency region between 220 and 565 GHz. A part of the transitions are illustrated in an energy diagram of figure 3.3. The ion was generated with a 1 : 3 mixture of D_2 and D_2O gases at a total pressure of 20 mTorr. When we set up the cell, the optimum condition for gas ratio and total pressure changed each time. The discharge current was 400 mA. The cell temperature was maintained between -10 and -40 °C.

The observed frequencies include ion-drift Doppler shifts since a relatively high voltage (a thousand volts) was applied to the discharge cell. The size of the shift was estimated by measuring the difference between the observed frequencies of the two strong lines at 455 GHz ($Q(J,K) = (4,3)$ and $(5,4)$) with normal and opposite electrode configurations, where microwave radiation was propagated from the anode to the cathode in the normal configuration and vice versa in the opposite. The difference between measured frequencies with both configurations was 160 kHz, and was used to correct observed line frequencies around 455 GHz; all other observed line frequencies were similarly corrected using the same proportionality factor. The rotational state dependency

of ionic mobilities was considered to be less than 10 % of the Doppler shifts [28,29]. This gives only uncertainties of about 16 kHz to the errors of the ion drift corrected frequencies. These uncertainties are comparable to or less than the frequency measurement errors in the present study (table I). The observed and ion-drift corrected frequencies are listed in table 1.

Relative intensities of the lines around 460 GHz were measured to determine an effective rotational temperature of D_3O^+ in the discharge. We used three transitions whose frequencies were close to each other. The relative intensities of $Q(J,K) = (1,1)$, $(2,2)$ and $(7,6)$ transitions were obtained to be $0.2_0 : 0.4_4 : 1.0_0$, respectively, from which the rotational temperature was estimated to be $500 \sim 600$ K with the assumption of a Boltzmann distribution of D_3O^+ in the related levels.

3.3 Molecular constants, structures and inversion potential

3.3.1 Determination of molecular constants

Q-branch transitions were observed up to the $J = K + 5$ series, but the observed lines could not be fitted without $\Delta k = \pm 3n$ interaction parameters. The analysis of the observed lines has to take account of the $\Delta k = \pm 3n$ interaction. A theory to deal with this interaction was developed to treat the pyramidal XY_3 type of molecule which has a large amplitude inversion motion such as NH_3 and H_3O^+ [23,24]. The forms of the operators, H_1 , H_2 and H_3 , describing the $\Delta k = \pm 3n$ interactions are given by equations (1a) - (1c):

$$H_1 = H_2(\rho)[(J_+^3 + J_-^3)J_z + J_z(J_+^3 + J_-^3)] \quad (1a)$$

$$H_2 = H_3(\rho)(J_+^3 - J_-^3) \quad (1b)$$

$$H_3 = [H_1(\rho) + H_4(\rho) + H_5(\rho)](J_+^6 + J_-^6) \quad (1c)$$

where $J_{\pm} = J_x \pm iJ_y$ (Symmetry of the operators are discussed in appendix I). $H_1(\rho)$ through $H_5(\rho)$ are functions of the inversion coordinate ρ and have been defined by equations (9a) - (9c) in [23]. The operators H_1 and H_2 mix the rotation-inversion wavefunctions $|\varphi; J, k\rangle$ and $|\varphi'; J, k \pm 3\rangle$ which have different symmetry with respect to inversion. The operator H_3 mixes the wavefunctions $|\varphi; J, k\rangle$ and $|\varphi; J, k \pm 6\rangle$ of the same symmetry for inversion.

Molecular constants were determined by a least-squares fit of the corrected frequencies to the following inversion-rotation energy formulas. The energy of the inversion-rotational levels was calculated from the Hamiltonian matrix. The diagonal elements of the matrix are described as

$$\begin{aligned} E(i)(J,K) = & E_0(i) + B(i)J(J+1) + (C-B)(i)K^2 \\ & - D_J(i)J^2(J+1)^2 - D_{JK}(i)J(J+1)K^2 - D_K(i)K^4 \\ & + H_J(i)J^3(J+1)^3 + H_{JK}(i)J^2(J+1)^2K^2 + H_{KJ}(i)J(J+1)K^4 + H_K(i)K^6 \end{aligned} \quad (2)$$

where i indicates the parity of inversion. We included the centrifugal distortion constants up to the sextic terms in this expression. The off-diagonal matrix elements are given by equations (3a) - (3c):

$$\begin{aligned} \langle \varphi(s); J, k | H_1 | \varphi(a); J, k \pm 3 \rangle \\ = \langle \varphi(a); J, k | H_1 | \varphi(s); J, k \pm 3 \rangle \\ = \alpha(2k \pm 3)F_{\pm 3}(J, k) \end{aligned} \quad (3a)$$

$$\begin{aligned} \langle \varphi(s); J, k | H_2 | \varphi(a); J, k \pm 3 \rangle \\ = - \langle \varphi(a); J, k | H_2 | \varphi(s); J, k \pm 3 \rangle = \pm \beta F_{\pm 3}(J, k) \end{aligned} \quad (3b)$$

$$\begin{aligned}
& \langle \varphi(s); J, k | H_3 | \varphi(s); J, k \pm 6 \rangle \\
& = \langle \varphi(a); J, k | H_3 | \varphi(a); J, k \pm 6 \rangle = \eta_3 F_{\pm 6}(J, k)
\end{aligned} \tag{3c}$$

where interaction parameters α , β , η_3 are centrifugal distortion constants and

$$F_{\pm n}(J, k) = \{[J(J+1) - k(k \pm 1)] \cdots [J(J+1) - (k \pm (n-1))(k \pm n)]\}^{1/2} \tag{4}$$

The interaction H_3 represents higher order centrifugal distortion effects. In the present fit, we considered the effects only for the $K = 3$ levels. There are two main reasons only $K = 3$ levels are effected the most strongly. First the equation (3c) term gives a diagonal contribution for $(J, 3)$ basis states resulting in a splitting of $K = 3$ levels. The relative intensity of the A_1 , A_2 splitting in the $Q(J, 3)$ transitions is 10:1 in A_1 and A_2 rotational species, respectively (see appendix II). However only one line was observed in each $Q(J, 3)$ transition. We assumed that all the lines were to be assigned to the A_1 components and that the A_2 components have negligible contribution to the spectra. The η_3 constant has two separate values, $\eta_3(0^+)$ and $\eta_3(0^-)$ in the inversion splitting. We treated the values of $\eta_3(i)$ as $\eta_3 (= (\eta_3(0^+) + \eta_3(0^-))/2)$. Secondly, the equations (3a) and (3b) terms are also expected to be larger for $K = 3$ levels, because of the close proximity of the $(J^+, 0)$ levels.

For $J = K + n$ ($n = 0, 1, 2, \cdots$) series lines of Q-branch, the off-diagonal matrix elements increase in the large n series lines, because $F_{\pm n}(J, k)$ in the equation (4) have a large value in the large n series line. Addition of the interaction parameters to the Hamiltonian proved to be essential to a good fit of the present data within their experimental errors, since the Q-branch transitions were considered up to the $J = K + 5$ series lines. Furthermore six combination differences (listed in table 1) in the 0^+ level were available from the data of the $\nu_2(1^- - 0^+)$ vibration bands which were calculated from the infrared data [19]. These data were weighted in the fit according to their experimental

uncertainties.

In the beginning the $\Delta k = \pm 3n$ interaction parameters were not included in the fit. The standard uncertainty converged to 3.8 MHz which is much larger than experimental uncertainty. Then α , β and η_3 were treated as free parameters in the fit. However, we found that one of two molecular constants, $(C - B)(0^+)$ and η_3 , had to be fixed in the fit, i.e. the two molecular constants could not be determined simultaneously. Finally η_3 was fixed at zero, and the standard uncertainty converged to 56.8 kHz. The interaction parameter α of D_3O^+ was roughly estimated to be approximately one-half of that of H_3O^+ ($\alpha = 2.7$ MHz [12]), and was determined to be 1.181(23) MHz which agrees with the estimated one. The constant C was determined to be 94390(1540) MHz in the 0^+ levels. This value agrees with 93300 MHz value reported by the theoretical calculation [21]. For the diagonal elements described in equation (2), the accurate ground-state inversion splitting was obtained to be 460346.410(32) MHz (15.35550338(107) cm^{-1}). The measurements of a number of Q-branch transitions with microwave spectroscopic precision resulted in this precise determination. The centrifugal distortion constant $D_{JK}(0^+)$ ($= -14.017(20)$ MHz) obtained in the present study differs significantly from the previously reported values, -22.60(66) [19] and -10.885(165) [20] MHz, which were obtained by the analysis of infrared data. The determined molecular constants are listed in table 2. The relatively large uncertainty, 56.8 kHz, may have some contributions from large line widths in the 400 to 500 GHz region (see figure 3.2) and/or the uncertainty of the Doppler shifts correction.

The experimental determination of the splitting in the zeroth vibrational level leads to a refinement of the splitting in the vibrationally excited state. Using infrared laser

spectroscopy, Petek *et al.* determined the $1^- - 0^+$ and the $1^+ - 0^-$ inversion components of the ν_2 band centers to be $645.13043(37)$ and $438.38619(61)$ cm^{-1} , respectively [20]. We calculated the splitting width for the ν_2 excited state to be $191.38874(98)$ cm^{-1} , where the error is mostly due to the experimental uncertainty of the infrared study. The determined inversion splittings are illustrated in double minimum potential of figure 3.4. The present result agrees well with the theoretically predicted value using the non-rigid inverter model, which varied from 15.2 to 15.7 cm^{-1} [19,21]. However, the potential function parameters can be revised using the present values of the two inversion splitting. The inversion splitting of the present study is essential for a deep understanding of the inversion potential of H_3O^+ .

3.3.2 Molecular structure of H_3O^+ and D_3O^+

The pyramidal symmetric-top molecule H_3O^+ has only two independent structural parameters, $r(\text{OH})$ and $\theta(\text{HOH})$, and can be determined from two rotational constants of one molecular species. The observed rotational constants only give the r_0 structure, which suffers from the effect of zero-point vibration and is physically uncertain in nature. The effect of zero-point vibrations for the symmetric XY_3 -type of molecule can be estimated by the standard method [30], as shown in the paper by Chu and Oka [31]. Since the rotational constants B_0 and C_0 in the 0^+ and 0^- levels of D_3O^+ have been determined in the present study, a precise structure can be derived from a combination of these constants and the previously determined rotational constants of H_3O^+ .

Using the nonrigid inverter Hamiltonian method, Špirko and Kraemer [21] determined an anharmonic potential, which fits well the experimental data for the lower

inversion and vibration states of H_3O^+ and D_3O^+ . Their “Fit I” parameters were used in the present study to calculate the vibration-rotation parameters. Zero-point corrections δB and δC for H_3O^+ and D_3O^+ are listed in table 3. Here, it was assumed that the hypothetical rotational constant of the inversionless ground level corresponds to the corresponding average values of the 0^+ and 0^- levels [32], as if the inversion splittings of H_3O^+ and D_3O^+ were extremely small and unobservable like those of SH_3^+ and PH_3 . We call its hypothetical level “ 0^0 ” in this paper. The rotational constant in the 0^0 levels, which is defined as $B_0(0^0) = (B_0(0^+) + B_0(0^-))/2$, was used to obtain an equilibrium structure (r_e structure) for H_3O^+ . The rotational constants B_0 and C_0 , and corrected ones B_z and C_z of the three levels (0^+ , 0^- and 0^0) for H_3O^+ and D_3O^+ are listed in table 3. Average structures (r_z structures) were derived straightforwardly from the two zero-point averaged rotational constants B_z and C_z . The calculated r_0 and r_z structures are listed in table 4.

In order to determine the r_e structure, the equilibrium rotational constants are indispensable. Generally they are derived from the rotational constants in the ground vibrational state and changes of rotational constants by excitation of each vibrational mode, which can be obtained from the measurements of spectral lines of molecules in the vibrationally excited states. However, it is not easy to determine changes of rotational constants by excitation of each vibrational mode for a polyatomic molecule having several modes. Contrary to this complex procedure a simpler method is to derive the r_e structure by extrapolating the r_z structure for isotopic species.

The determined r_z structure in the 0^0 level of D_3O^+ differs from that of H_3O^+ by 0.0046(25) Å. This difference is due to the anharmonicity in the stretching vibrations and the reduced masses in H_3O^+ and D_3O^+ , which can be related to the r_e structure by using a

diatomic approximation due to Oka and Morino [33],

$$r_z - r_e = -3\hbar F_3 / 4\sqrt{\mu F_2^3} \quad (5)$$

where F_2 and F_3 are diatomic molecular potential constants defined by

$$2U(r) = F_2(r - r_e)^2 + F_3(r - r_e)^3 + \dots, \quad (6)$$

and μ is the reduced mass of two atoms. The difference between r_z and r_e is inversely proportional to the square root of μ , and the procedure of extrapolation is described in figure 3.5. A similar relation is assumed to hold in the difference between θ_z and θ_e . The r_e structure was calculated to be $r_e = 0.9702(89)\text{\AA}$ and $\theta_e = 109.4(38)^\circ$. The determined r_e structure for H_3O^+ is listed together with the reported theoretical values in table 5. The F_2 and F_3 values of H_3O^+ are estimated by using Herschbach and Laurie's empirical relation [34]: $F_2 = 8.36 \times 10^5 \text{ dyn cm}^{-1}$ and $F_3 = -9.15 \times 10^{13} \text{ dyn cm}^{-2}$, which give $r_z(\text{OH}) - r_z(\text{OD})$ to be 0.0021\AA . This value is smaller than 0.0046\AA derived from the r_z structures by using the potential function parameters in Fit I for H_3O^+ [21]. The present bond angle of the r_e structure agrees with the theoretical one, though the uncertainty is large. The bond length in [19] corresponds to the present one. However the bond length in [21] are outside of one standard error of the present one. The potential function parameters may be refined with use of the inversion-splittings of the ground state and the ν_2 inversion state.

3.3.3 $\Delta K = 3$ forbidden transitions

The $\Delta k = \pm 3n$ interaction mixes the (J^\pm, K) and $(J^\mp, K \pm 3n)$ rotational levels. The strongest mixing of D_3O^+ occurs between the $(J^+, 0)$ and $(J^-, 3)$ levels. The $(J^+, 0) - (J^-, 3)$ forbidden transition, $\Delta K = 3$, obtains an intensity from the $(J^-, 3) - (J^-, 3)$ normally

allowed transition, $\Delta K = 0$, as rotational intensity borrowing. The $\Delta K = 3$ forbidden transition gains intensity due to this mixing. Frequencies of the forbidden transitions were predicted by the present molecular constants and the intensities were also calculated from the coefficients of the mixing of wave functions. For example the $(3^+, 0) - (3^+, 3)$ transition is located at 680.7(139) GHz where the large uncertainty mostly comes from the uncertainty of the constant C . However the relative intensities of the corresponding $\Delta K = 0$ Q-branch transitions, i.e. $I[(J^+, 0) - (J^+, 3)] / I[(J^-, 3) - (J^-, 3)]$, are 10^{-3} to 10^{-4} % in $J = 3$ to 8 transitions. A trial survey search for the forbidden transition was not successful.

3.3.4 Rotational constants of H_2DO^+

The H_2DO^+ ion is of particular interest to interstellar chemistry, since it is considered to play an important role in deuterium fractionation of related interstellar molecules, H_2O , OH [35]. Detection of H_2DO^+ in interstellar clouds with radio telescopes would provide a value for the $[\text{H}_2\text{DO}^+]/[\text{H}_3\text{O}^+]$ ratio which may be important in assessing a proposed reaction scheme for OH, H_2O and H_3O^+ .

A plausible prediction of the spectral pattern for H_2DO^+ can be derived from a reasonable molecular structure. The r_z rotational constants for the 0^+ and 0^- states were calculated by using the OH and OD r_z bond lengths and $\angle\text{H-O-axis}$ and $\angle\text{D-O-axis}$ for H_3O^+ and D_3O^+ , where “axis” means the molecular axis of H_3O^+ and D_3O^+ . Then the zero-point average corrections were made for the r_z rotational constants, giving a set of the r_0 rotational constants as listed in table 6. The uncertainties of the rotational constants were due to the uncertainties in the r_z structure of H_3O^+ and D_3O^+ . These rotational constants together with an expected inversion splitting can provide spectral line frequencies for the

inversion-rotation transitions for H_2DO^+ , which are useful for both laboratory and astronomical spectroscopy.

Appendix I

The wavefunction $\varphi(s)$ and $\varphi(a)$ in the D_{3h} symmetry of H_3O^+ are of the symmetry species A_1' and A_2'' , respectively. Let us consider following matrix elements:

$$\langle \varphi(s) | H | \varphi(a) \rangle \text{ and } \langle \varphi(a) | H | \varphi(s) \rangle, \quad (i)$$

$$\langle \varphi(s) | H | \varphi(s) \rangle \text{ and } \langle \varphi(a) | H | \varphi(a) \rangle. \quad (ii)$$

So as to have a nonzero value in the matrix elements, their symmetry must be a totally symmetry species A_1' , i.e. the symmetry species of the Hamiltonian H must be including the symmetry species A_2'' and A_1' in the matrix elements (i) and (ii), respectively. The symmetry species of the operators and of the wavefunctions in the D_{3h} symmetry of the pyramidal XY_3 molecule were described in [36,37]. From the relations, the symmetry species of the operators in the equations (1a) - (1c) are obtained as follows:

$$\begin{aligned} H_2(\rho) &: A_2'', \\ H_3(\rho) &: A_2'', \\ H_1(\rho) + H_4(\rho) + H_5(\rho) &: A_1', \\ (\mathcal{J}_+^3 + \mathcal{J}_-^3)J_z + J_z(\mathcal{J}_+^3 + \mathcal{J}_-^3) &: A_1'' + A_2'' + E'', \\ (\mathcal{J}_+^3 - \mathcal{J}_-^3) &: A_1'' + A_2'' + E'', \\ (\mathcal{J}_+^6 + \mathcal{J}_-^6) &: A_1' + A_2' + E'. \end{aligned}$$

As a result, the symmetry species of the operators H_1 , H_2 and H_3 are indicated to be $A_1' + A_2' + E'$, and the matrix elements in the equations (3a) - (3c) may have nonzero values.

Appendix II

Symmetry species of the inversion-rotation energy levels in the nondegenerate vibrational states of D_3O^+ (in the D_{3h} group) are given in following table. Spin statistical weight in the A_1' , A_2'' , A_2' , A_1'' , E' , E'' symmetry species are 10, 1, 1, 10, 8, 8, respectively.

$ J, k\rangle$	J even		J odd	
	+	-	+	-
$ J, 0\rangle$	A_1'	A_2''	A_2'	A_1''
$ J, 1\rangle, J, -1\rangle$	E''	E'	E''	E'
$ J, 2\rangle, J, -2\rangle$	E'	E''	E'	E''
$ J, 3\rangle + J, -3\rangle$	A_1''	A_2'	A_2''	A_1'
$ J, 3\rangle - J, -3\rangle$	A_2''	A_1'	A_1''	A_2'
$ J, 4\rangle, J, -4\rangle$	E'	E''	E'	E''
$ J, 5\rangle, J, -5\rangle$	E''	E'	E''	E'
$ J, 6\rangle + J, -6\rangle$	A_1'	A_2''	A_2'	A_1''
$ J, 6\rangle - J, -6\rangle$	A_2'	A_1''	A_1'	A_2''

References

- [1] BEGEMANN, M. H., GUDEMAN, C. S., PFAFF, J., and SAYKALLY, R. J., 1983, *Phys. Rev. Lett.*, **51**, 554.
- [2] BEGEMANN, M. H., and SAYKALLY, R. J., 1985, *J. chem. Phys.*, **82**, 3570.
- [3] HAESE, N. N., and OKA, T., 1984, *J. chem. Phys.*, **80**, 572.
- [4] LEMOINE, B., and DESTOMBES, J. L., 1984, *Chem. Phys. Lett.*, **111**, 284.
- [5] LIU, D. -J., HAESE, N. N., and OKA, T., 1985, *J. chem. Phys.*, **82**, 5368.
- [6] DAVIES, P. B., HAMILTON, P. A., and JOHNSON, S. A., 1985, *J. Opt. Soc. Am.*, **B2**, 794.
- [7] LIU, D. -J., and OKA, T., 1985, *Phys. Rev. Lett.*, **54**, 1787.
- [8] PLUMMER, G. M., HERBST, E., and DELUCIA, F. C., 1985, *J. chem. Phys.*, **83**, 1428.
- [9] LIU, D. -J., OKA, T., and SEARS, T. J., 1986, *J. chem. Phys.*, **84**, 1312.
- [10] BOGEY, M., DEMUYNCK, C., DEMIS, M., and DESTOMBES, J. L., 1985, *Astron. Astrophys.*, **148**, L11.
- [11] VERHOEVE, P., TERMEULEN, J. J., MEERTS, W. L., and DYMANUS, A., 1988, *Chem. Phys. Lett.*, **143**, 501.
- [12] VERHOEVE, P., VERSLUIS, M., TERMEULEN, J. J., MEERTS, W. L., and DYMANUS, A., 1989, *Chem. Phys. Lett.*, **161**, 195.
- [13] ŠPIRKO, V., and BUNKER, P. R., 1982, *J. molec. Spectrosc.* **95**, 226.
- [14] BUNKER, P. R., KRAEMER, W. P., and SPIRKO, V., 1983, *J. molec. Spectrosc.* **101**, 180.
- [15] BOTSCHWINA, P., ROSMUS, P., and REINSCH, E. -A., 1983, *Chem. Phys. Lett.* **102**, 299.

- [16] SHIDA, N., TANAKA, K., and OHNO, K., 1984, *Chem. Phys. Lett.* **104**, 575.
- [17] BUNKER, P. R., AMANO, T., and SPIRKO, V., 1984, *J. molec. Spectrosc.* **107**, 208.
- [18] DANIELIS, V., and SPIRKO, V., 1986, *J. molec. Spectrosc.* **117**, 175.
- [19] SEARS, T. J., BUNKER, P. R., DAVIES, P. B., JOHNSON, S. A., and ŠPIRKO, V., 1985, *J. chem. Phys.*, **83**, 2676.
- [20] PETEK, H., NESBITT, D. J., OWRUTSKY, J. C., GUDEMAN, C. S., YANG, X., HARRIS, D. O., MOORE, C. B., and SAYKALLY, R. J., 1990, *J. chem. Phys.*, **92**, 3257.
- [21] ŠPIRKO, V., and KRAEMER, W. P., 1989, *J. molec. Spectrosc.*, **134**, 72.
- [22] ALIEV, M. R., and WATSON, J. K. G., 1976, *J. molec. Spectrosc.*, **61**, 29.
- [23] BELOV, S. P., GERSHSTEIN, L. I., KRUPNOV, A. F., MASLOVSKIĬ, A. V., URBAN, S., ŠPIRKO, V., and PAPOUŠEK, D., 1980, *J. molec. Spectrosc.*, **84**, 288.
- [24] URBAN, Š., ŠPIRKO, V., PAPOUŠEK, D., KAUPPINEN, J., BELOV, S. P., GERSHSTEIN, L. I., and KRUPNOV, A. F., 1981, *J. molec. Spectrosc.*, **88**, 274.
- [25] UY, D., WHITE, E. T., and OKA, T., 1997, *J. molec. Spectrosc.*, **183**, 240.
- [26] SAITO, S., KAWAGUCHI, K., and HIROTA, E., 1985, *J. chem. Phys.* **82**, 45.
- [27] KAWAGUCHI, K., YAMADA, C., SAITO, S., and HIROTA, E., 1985, *J. chem. Phys.* **82**, 1750.
- [28] HAESE, N. N., PAN, F.-S., and OKA, T., 1983, *Phys. Rev. Lett.* **50**, 1575.
- [29] GUDEMAN, C. S., and SAYKALLY, R. J., 1984, *Ann. Rev. phys. Chem.* **35**, 387.
- [30] OKA, T., 1960, *J. phys. Soc. Jpn.*, **15**, 2274.
- [31] CHU, F. Y., and OKA, T., 1974, *J. chem. Phys.*, **60**, 4612.
- [32] BENEDICT, W. S., and PLYLER, E. K., 1957, *Can. J. Phys.*, **35**, 1235.

- [33] OKA, T., and MORINO, Y., 1962, *J. molec. Spectrosc.*, **8**, 300.
- [34] HERSCHBACH, D. R., and LAURIE, V. W., 1961, *J. chem. Phys.*, **35**, 458.
- [35] WATSON, W. D., 1976, *Rev. mod. Phys.*, **48**, 513.
- [36] PAPOUŠEK, D., STONE, J. M. R., and ŠPIRKO, V., 1973, *J. molec. Spectrosc.* **48**, 17.
- [37] ŠPIRKO, V., STONE, J. M. R., and PAPOUŠEK, D., 1976, *J. molec. Spectrosc.* **60**, 159.

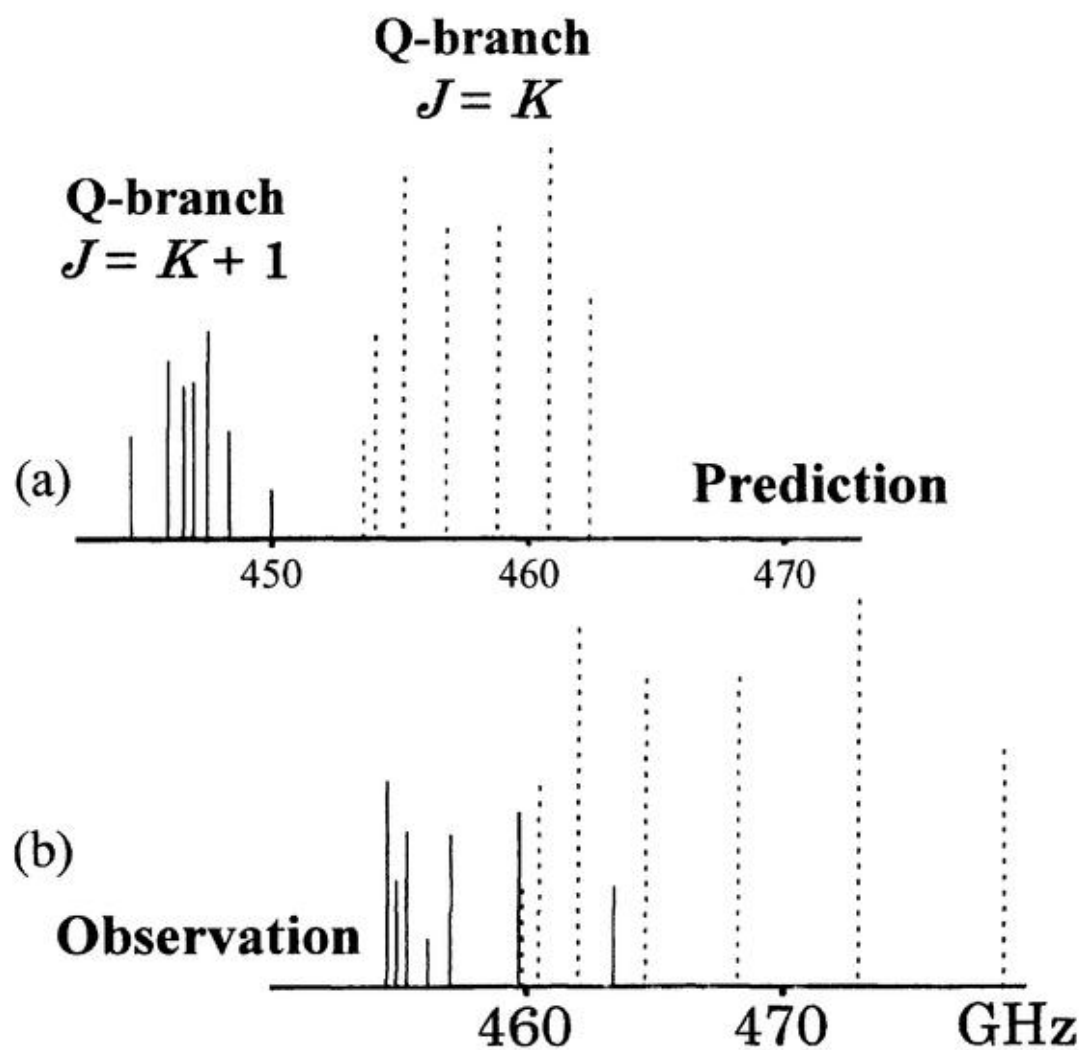


Figure 3.1. Stick diagrams of the predicted (a) and observed (b) spectra. The solid sticks denote the $J = K + 1$ series lines of Q-branch transition while the broken sticks denote the $J = K$ ones. The intensity of the lines depend on nuclear spin weight and a Boltzmann distribution.

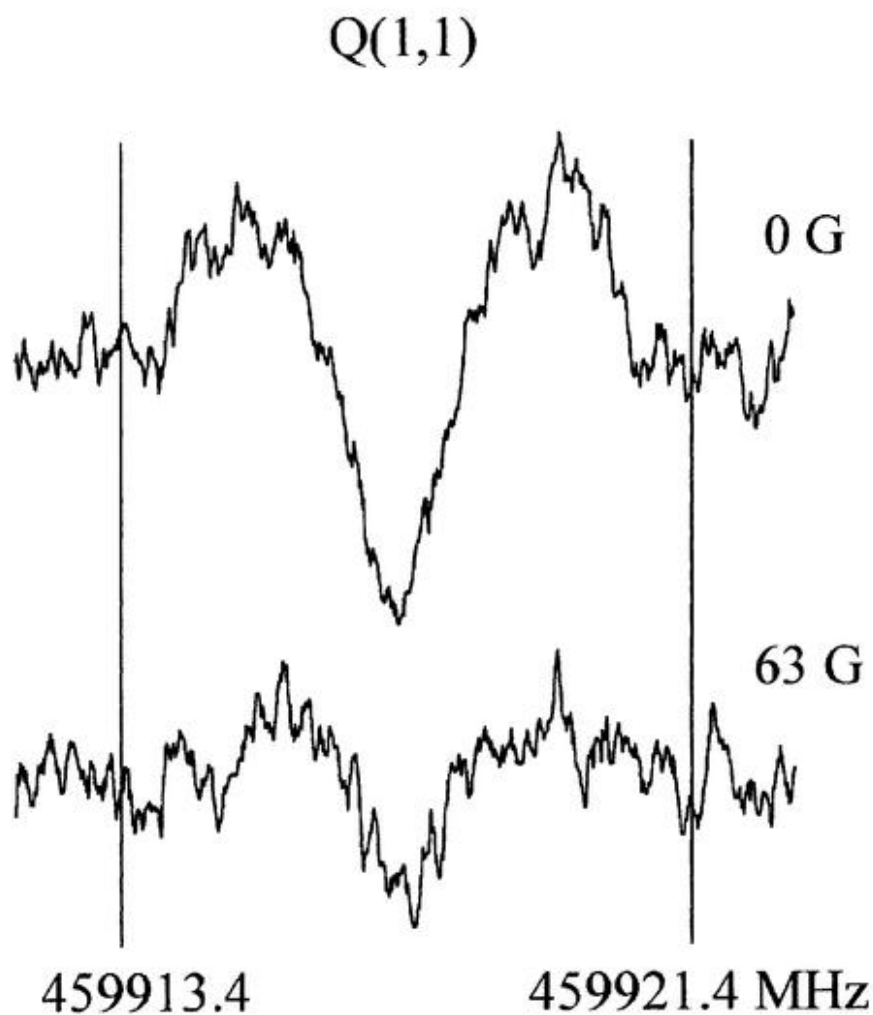
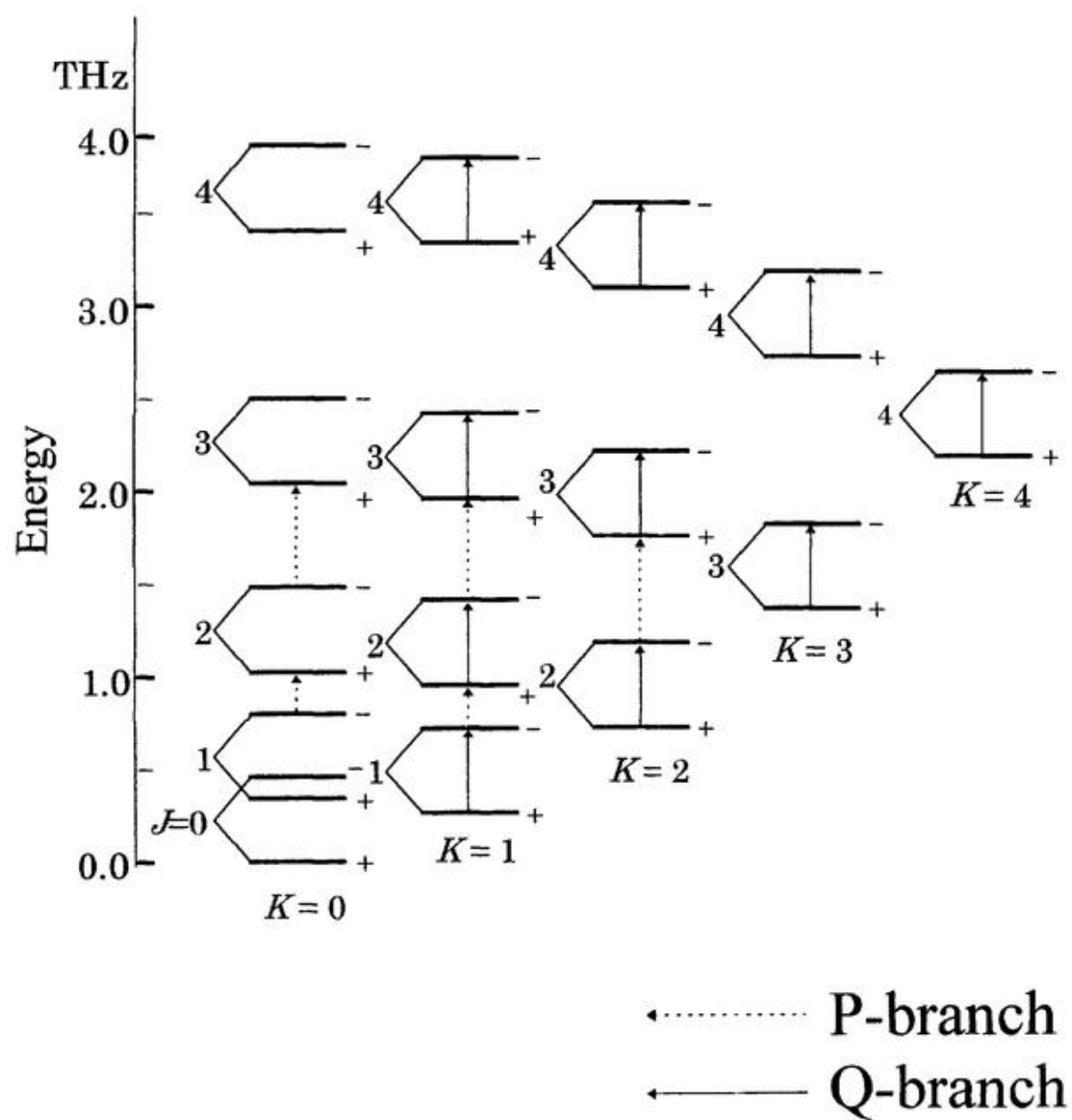


Figure 3.2. The $Q(1, 1)$ transition of D_3O^+ obtained with an integration time of 290 s (1600 scans). The upper trace was obtained without a magnetic field, whereas a field of 63 gauss was applied in recording the lower trace. The large line width of D_3O^+ occurred mainly due to pressure broadening.

Figure 3.3. Energy diagram of D_3O^+ and the observed P- and Q-branch transitions.

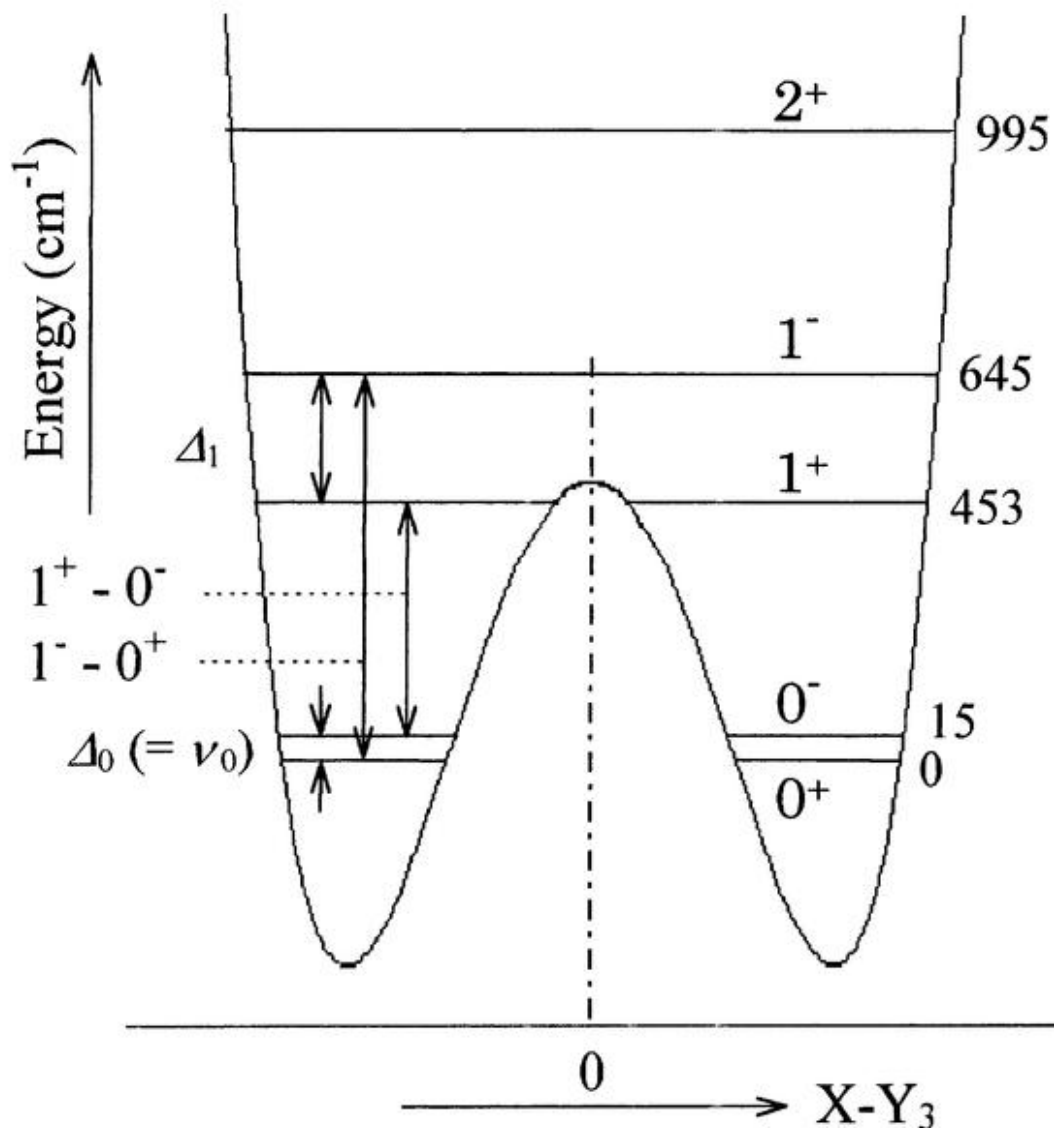


Figure 3.4. The determined splitting width of the ground state and the ν_2 excited state for D_3O^+ . $\Delta_0 (= \nu_0)$ and Δ_1 indicate the splitting width of the ground state and the ν_2 excited state, respectively. The $1^- - 0^+$ and the $1^+ - 0^-$ inversion components of the ν_2 band were determined to be 645.13043(37) and 438.38619(61) cm^{-1} , respectively, by infrared laser spectroscopy [20]. We calculated the splitting width for the ν_2 excited state to be 191.38874(98) cm^{-1} .

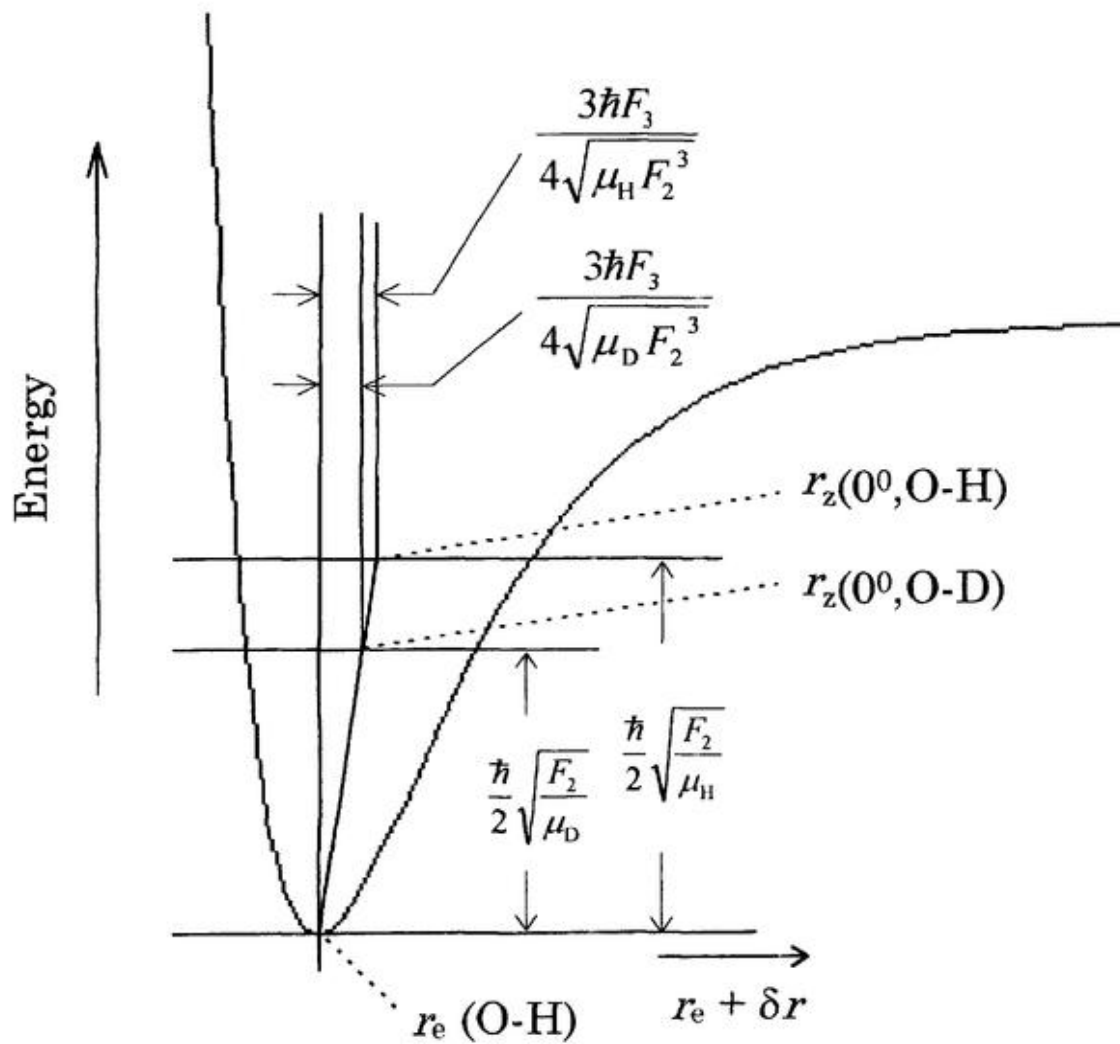


Figure 3.5. Extrapolation from r_z to r_e .

Table 1. Rotational-inversion frequencies (in MHz) for D_3O^+ .

$J'^{-} - J'^{+}$	K	$\nu_{\text{obs.}}^{\text{b}}$	$\nu_{\text{corr.}}^{\text{c}}$	$\Delta\nu^{\text{d}}$
1 ⁻ 1 ⁺	1	459917.791(38)	459917.710	0.052
2 ⁻ 2 ⁺	2	460493.132(14)	460493.051	-0.029
3 ⁻ 3 ⁺	3	462074.692(7)	462074.611	-0.007
4 ⁻ 4 ⁺	4	464669.162(15)	464669.080	-0.009
5 ⁻ 5 ⁺	5	468288.635(15)	468288.552	0.008
6 ⁻ 6 ⁺	6	472949.967(13)	472949.884	-0.016
7 ⁻ 7 ⁺	7	478675.348(13)	478675.264	0.042
8 ⁻ 8 ⁺	8	485491.826(10)	485491.741	0.001
2 ⁻ 2 ⁺	1	456211.479(12)	456211.399	-0.041
3 ⁻ 3 ⁺	2	454940.389(14)	454940.309	-0.024
4 ⁻ 4 ⁺	3	454664.410(17)	454664.331	0.052
5 ⁻ 5 ⁺	4	455380.853(16)	455380.774	0.008
6 ⁻ 6 ⁺	5	457089.243(19)	457089.163	-0.009
7 ⁻ 7 ⁺	6	459795.652(12)	459795.571	-0.066
8 ⁻ 8 ⁺	7	463510.799(12)	463510.718	-0.060
10 ⁻ 10 ⁺	9	474033.831(15)	474033.748	-0.304 ^e
11 ⁻ 11 ⁺	10	480887.578(21)	480887.494	-0.520 ^e
12 ⁻ 12 ⁺	11	488841.778(38)	488841.692	-0.724 ^e
3 ⁻ 3 ⁺	1	450709.821(103)	450709.742	-0.069
4 ⁻ 4 ⁺	2	447644.166(11)	447644.087	0.064
5 ⁻ 5 ⁺	3	455575.551(24)	455575.473	0.071
6 ⁻ 6 ⁺	4	444486.711(27)	444486.633	0.032
7 ⁻ 7 ⁺	5	444371.033(22)	444370.955	0.04
8 ⁻ 8 ⁺	6	445222.186(22)	445222.108	0.073
9 ⁻ 9 ⁺	7	447040.045(20)	447039.966	0.150 ^f
10 ⁻ 10 ⁺	8	449828.921(49)	449828.843	-0.024 ^e
11 ⁻ 11 ⁺	9	453598.881(20)	453598.801	0.281 ^e
12 ⁻ 12 ⁺	10	458363.458(8)	458363.377	0.577 ^e
5 ⁻ 5 ⁺	2	438693.386(30)	438693.309	0.026
6 ⁻ 6 ⁺	3	434906.802(15)	434906.726	-0.090
7 ⁻ 7 ⁺	4	432114.696(12)	432114.620	-0.032
8 ⁻ 8 ⁺	5	430280.020(17)	430279.944	-0.042
9 ⁻ 9 ⁺	6	429392.353(16)	429392.277	-0.026

10 ⁻	10 ⁺	7	429441.397(16)	429441.321	0.016
11 ⁻	11 ⁺	8	430421.494(17)	430421.418	-0.023
12 ⁻	12 ⁺	9	432331.925(35)	432331.849	0.037
13 ⁻	13 ⁺	10	435176.151(7)	435176.075	-0.012
6 ⁻	6 ⁺	2	428196.019(21)	428195.944	-0.006
7 ⁻	7 ⁺	3	422811.477(21)	422811.403	0.000
8 ⁻	8 ⁺	4	418406.534(32)	418406.460	-0.208 ^c
9 ⁻	9 ⁺	5	414973.327(9)	414973.254	-0.197 ^c
10 ⁻	10 ⁺	6	412477.388(50)	412477.316	0.006
11 ⁻	11 ⁺	7	410898.424(16)	410898.351	0.004
12 ⁻	12 ⁺	8	410221.569(19)	410221.497	-0.010
13 ⁻	13 ⁺	9	410435.957(29)	410435.885	-0.574 ^c
8 ⁻	8 ⁺	3	409359.903(16)	409359.831	0.021
9 ⁻	9 ⁺	4	403515.149(31)	403515.078	0.419 ^c
10 ⁻	10 ⁺	5	398616.689(19)	398616.619	1.284 ^c
2 ⁺	1 ⁻	0	221760.208(12)	221760.169	0.059
2 ⁺	1 ⁻	1	220397.505(23)	220397.466	-0.060
3 ⁺	2 ⁻	0	565066.727(29)	565066.628	0.007
3 ⁺	2 ⁻	1	563748.641(36)	563748.542	-0.023
3 ⁺	2 ⁻	2	559770.314(29)	559770.216	0.017
8 ⁺	7 ⁺	6		2714369	188 ^{c,g}
7 ⁺	6 ⁺	6		2378622	48 ^{g,h}
6 ⁺	5 ⁺	4		2037351	-41 ^{g,h}
4 ⁺	3 ⁺	3		1360071	4 ^{g,h}
3 ⁺	2 ⁺	2		1020224	-39 ^{g,h}
5 ⁺	4 ⁺	2		1697704	4 ^{g,h}

^a The sign i expresses levels of the inversion splitting, where + and - signs indicate lower and upper levels and correspond to s and a in [20].

^b Values in parentheses denote one standard deviation of the frequency measurement and apply to the last digits of the frequencies.

^c Observed frequencies corrected by the ion-drift Doppler shift. The values were used in the least squares fit. All lines given a weigh of 1.0 except where otherwise stated.

^d $\Delta\nu = \nu_{\text{corr.}} - \nu_{\text{calc.}}$

^e Not included in the least squares fit.

^f Weight is 0.1.

^g Combination differences calculated from infrared data [19].

^h Weight is 0.16×10^{-5} .

Table 2. Molecular constants of the $\nu = 0^+, 0^-$ levels of D_3O^+ (MHz).

$\nu(0^+ - 0^-)$	460346.410(32)		
$B(0^+)$	170130.218(24)	ΔB	-931.4421(37)
$(C - B)(0^+)$	-75740(1540)	$\Delta(C - B)$	1433.8794(61)
$D_J(0^+)$	8.53866(152)	ΔD_J	-0.971602(130)
$D_{JK}(0^+)$	-16.887(20)	ΔD_{JK}	2.87030(46)
$D_K(0^+)$	10.409 ^b	ΔD_K	-2.10700(46)
$H_J(0^+)$	0.0 ^c	ΔH_J	-0.0006465(21)
$H_{JK}(0^+)$	-0.00512(178)	ΔH_{JK}	0.0027678(79)
$H_{KJ}(0^+)$	0.0115(39)	ΔH_{KJ}	-0.0038841(106)
$H_K(0^+)$	0.0 ^c	ΔH_K	0.0017902(65)
α	1.181(23)	η_3	0.0 ^c
β	-0.302(45)		

^a Values in parentheses denote the one standard deviation, and apply to the last digits of the constants.

^b Fixed at experimental value from [20].

^c Fixed.

Table 3. Zero-point average rotational constants and corrections of H_3O^+ and D_3O^+ (MHz).^a

	$\text{H}_3\text{O}^+(0^+)^b$	$\text{H}_3\text{O}^+(0^-)^b$	$\text{D}_3\text{O}^+(0^+)$	$\text{D}_3\text{O}^+(0^-)$
B_0	337400.22(39)	331411.69(69)	170130.218(24)	169198.776(28)
B_z	330969(64)	324980(65)	167771(24)	166840(24)
C_0	184241(60)	186711(60)	94390(1540)	94890(1540)
C_z	182912(73)	185381(73)	93930(1540)	94440(1540)
$B_0(0^0)^c$	334405.96(54)		169664.479(26)	
$B_z(0^0)^c$	327975(65)		167306(24)	
$C_0(0^0)^c$	185476(60)		94640(1540)	
$C_z(0^0)^c$	184147(73)		94180(1540)	
δB^d	-6431(64)		-2359(24)	
δC^d	-1329(13.3)		-456.5(4.5)	

^a Values in parentheses are one standard deviation and apply to the last digits of the constants.

^b B_0 and C_0 of H_3O^+ from [12] and [25], respectively.

^c Estimated rotational constants in the 0^0 level, see text.

^d The uncertainties in the zero-point corrections of rotational constants estimated to be 1%.

Table 4. Molecular structure of H_3O^+ and D_3O^+ .^a

		Effective (r_0)	Average (r_z) ^b
$\text{H}_3\text{O}^+(0^+)$	$r(\text{\AA})$	0.978229(62)	0.985419(134)
	$\alpha(^{\circ})$	114.9680(181)	114.307(32)
$\text{H}_3\text{O}^+(0^-)$	$r(\text{\AA})$	0.981178(60)	0.988525(135)
	$\alpha(^{\circ})$	113.2585(175)	112.587(32)
$\text{D}_3\text{O}^+(0^+)$	$r(\text{\AA})$	0.9762(23)	0.9818(23)
	$\alpha(^{\circ})$	113.25(99)	112.68(100)
$\text{D}_3\text{O}^+(0^-)$	$r(\text{\AA})$	0.9774(22)	0.9830(23)
	$\alpha(^{\circ})$	112.58(98)	112.02(100)
$\text{H}_3\text{O}^+(0^0)^c$	$r(\text{\AA})$		0.986939(134)
	$\alpha(^{\circ})$		113.443(32)
$\text{D}_3\text{O}^+(0^0)^c$	$r(\text{\AA})$		0.9824(23)
	$\alpha(^{\circ})$		112.35(100)

^a Values in parentheses are one standard deviation and apply to the last digits of the constants.

^b The error of the r_z structure was caused by the uncertainties in the zero-point corrections of rotational constants. The uncertainties were estimated to be 1% of the correction.

^c Molecular structures in the 0^0 level, see text.

Table 5. Equilibrium structure of H_3O^+ .^a

	$r (\text{\AA})$	$\alpha (^\circ)$
Present	0.9702(89)	109.4(38)
Fit I in [21] ^b	0.9857	111.8
Fit II in [21] ^b	0.9855	112.0
[19] ^b	0.9758	111.3

^a Values in parentheses are one standard deviation and apply to the last digits of the constants.

^b Calculated by theoretical method.

Table 6. Predicted rotational constants of H_2DO^+ (GHz).^a

	0^+	0^-
A_0	329.0(21)	324.0(21)
B_0	212.11(103)	209.98(101)
C_0	140.50(82)	141.93(85)

^a Values in parentheses are one standard deviation and apply to the last digits of the constants.

4. Microwave Spectrum of the SD_3^+ Ion: Molecular Structure

[*Journal of Molecular Spectroscopy*, **192**, 228 (1998)]

4.1 Introduction

The gaseous SH_3^+ ion was first studied by Nakanaga and Amano [1,2] who reported the ν_1 and ν_3 fundamental bands studied with use of a difference frequency laser spectrometer combined with a hollow-cathode discharge cell. They determined the r_0 structure of SH_3^+ from observed rotational constants B_0 and C_0 . Later, the ν_2 fundamental band of SH_3^+ was studied with infrared diode laser spectroscopy [3]. On the basis of the molecular constants determined from the infrared spectroscopy, the lowest two rotational transitions of SH_3^+ were observed at 293 and 587 GHz [4,5]. The rotational constant B_0 and the centrifugal distortion constants D_J and D_{JK} were revised. Various physical properties have been predicted by many theoretical studies [6-13]. Particularly, equilibrium geometry, vibrational frequencies, force field, and rotational, centrifugal distortion and Coriolis coupling constants were predicted by Botschwina and his collaborators using a high-level *ab initio* calculation [13].

We measured rotational spectral lines of SD_3^+ by using microwave spectroscopy. Combined with the previously reported rotational constants of SH_3^+ the determined rotational constant was used to derive the molecular structure of SH_3^+ . When we finished the preparation of the manuscript for this study, we noticed that Xia *et al.* [14] reported an infrared diode laser study of the ν_1 and ν_3 bands.

4.2 Experimental

As described in chapter 2, the SD_3^+ ion was produced in the free-space absorption

cell with the hollow-cathode discharge in a mixture of D_2S and D_2 . The optimum condition used for SH_3^+ [5] was employed in the present study where the partial gas pressures were 5 mTorr of D_2S and 10 mTorr of D_2 , and a discharge current was 500 mA. The cell temperature was maintained at -150 to -190°C .

The SH_3^+ ion is an oblate symmetric-top molecule with C_{3v} symmetry. Prior to observations of SD_3^+ spectral lines, the rotational constant of SD_3^+ was estimated. The r_0 structure of SH_3^+ was calculated from B_0 [5] and C_0 [2] as $r_0 = 1.3578717(57) \text{ \AA}$ and $\theta_0 = 94.17252(108)^\circ$. Shifts of the SH bond length r_0 and HSH bond angle θ_0 by deuterium substitution were assumed to be the same as those of the isoelectronic molecule PH_3 : $\Delta r_0 = -0.0024 \text{ \AA}$ and $\Delta \theta_0 = 0.014^\circ$ [2,15]. The rotational constant B_0 of SD_3^+ was calculated to be 76245 MHz from the estimated molecular structure under this assumption.

We observed two lines near the predicted frequencies of $J = 2 - 1$ in the 305 GHz region. A separation of 6.3 MHz between the two lines agrees well with 6.0 MHz for the separation between the $K = 0$ and 1 lines, predicted from a value of D_{JK} , -1.499 MHz, by *ab initio* calculation [13], and their relative intensity also agrees with an expected one:

$$I(K = 0):I(K = 1) = 11:12.$$

The two lines showed similar chemical behavior. The intensity of the two lines decreased by a factor of 3 to 4 when an external magnetic field of 88 G was applied to the cell [4]. Furthermore the two lines showed relatively large line widths and their intensities were approximately in proportion to the discharge current. The observed lines were thus confirmed to be those of SD_3^+ . Successively the lines of $J = 1 - 0$, $3 - 2$, and $4 - 3$ were also observed at the expected frequencies and the lines showed also the same chemical behavior. The line frequencies were determined by averaging five pairs of successive up-

and down-ward scans.

4.2.1 Ion-drift Doppler shift correction

The observed frequencies include ion-drift Doppler shift. The shift was estimated by measuring a difference between the observed frequencies of the $J, K = 3, 2 - 2, 2$ transition at 364.8 GHz of H_3O^+ with normal and opposite electrode configuration, where microwave radiation was propagated from the anode side to the cathode side in the normal configuration and vice versa in the opposite one. The experimental condition was maintained as that of SD_3^+ . The measured difference were 0.07₈ MHz. Since the Doppler shift $\Delta\nu$ is given by ν/\sqrt{M} where ν is frequency and M molecular weight, the corresponding shift of the SD_3^+ spectral lines is calculated to be $\Delta\nu = 7.4 \times 10^{-8} \nu$ MHz. The observed frequencies were corrected by using this relation. The transition frequencies of the $J = 1 - 0$ to $4 - 3$ in the frequency region of 150 to 600 GHz are listed in table 1, and the observed transitions are illustrated in energy diagram of SD_3^+ as shown in figure 4.1. An example of observed spectral lines is shown in figure 4.2.

4.3 Molecular structure

The rotational constant and centrifugal distortion constants were determined from ten observed frequencies with a method of least squares fitting. The standard deviation of the fit was 39.1 kHz. An inclusion of the higher-order centrifugal distortion constants H_J , H_{JK} and H_{KJ} were found to be unnecessary in the fit. The rms value obtained in the present study is somewhat large. Symmetrical line shapes for most of the observed lines suggest that contributions of hyperfine structure due to electric quadrupole interaction of the

deuterium nucleus and inversion doubling are small and not observable in the present study. A pyramidal inversion barrier of SH_3^+ is predicted to be 34.8 kcal/mol, which may give a very small doubling to rotational levels of the ground vibrational state [6]. The relatively large rms is considered to be due to large spectral line widths, as demonstrated in figure 4.2. The determined molecular constants are listed in table 2, where the constants reported by infrared spectroscopy [14] and predicted by the theoretical study [13] are also shown for comparison. The present molecular constants agree well with those given by infrared spectroscopy and also by the theoretical study.

4.3.1 r_z structure

There are only two independent structural parameters, $r(\text{SH})$ and $\theta(\text{HSH})$, for SH_3^+ . Generally the observed rotational constants include the effect of zero-point vibration, which can be estimated by the standard method [16], as shown in the paper by Chu and Oka [17]. Since the rotational constant B_0 of SD_3^+ has been precisely determined in the present study, a combination of this constant and the previously determined rotational constants of SH_3^+ gives a precise structure.

Three fundamental bands of SH_3^+ and several vibration-rotation constants were reported [2,3] and well explained by a force field predicted by Botschwina and his collaborators [13] using an *ab initio* calculation. This was used to calculate the vibration-rotation parameters. Zero-point corrections for SH_3^+ and SD_3^+ are listed in table 3. The r_z structure of SH_3^+ is derived straight from two zero-point averaged rotational constants (table 4). The C_0 rotational constant was reported to be 63.62(117) GHz by Xia *et al.* [14], but the error associated with the constant is larger than its zero-point correction. Therefore,

only one corrected rotational constant can be used for the determination of the r_z structure for SD_3^+ . To obtain a reasonable r_z structure for SD_3^+ , the same difference found for $\theta_z(\text{PH}_3)$ and $\theta_z(\text{PD}_3)$ [15] was assumed between $\theta_z(\text{SH}_3^+)$ and $\theta_z(\text{SD}_3^+)$. Thus $r_z(\text{SD}_3^+)$ was determined to be $1.36086(16) \text{ \AA}$, which differs from $r_z(\text{SH}_3^+)$ by $0.00426(38) \text{ \AA}$.

4.3.2 r_e structure

The difference is due to the anharmonicity in stretching vibration and the difference of reduced masses in SH_3^+ and SD_3^+ , which can be related to r_e by using a diatomic approximation [18] (see equations (6) and (7) in chapter 3),

$$r_z - r_e = -3\hbar F_3 / 4\sqrt{\mu F_2^3}, \quad (1)$$

where F_2 and F_3 are diatomic molecular potential constants defined by

$$2U(r) = F_2(r - r_e)^2 + F_3(r - r_e)^3 + \dots, \quad (2)$$

and μ is the reduced mass of two atoms. The difference between r_z and r_e is inversely proportional to square root of μ . A similar relation was assumed in the difference between θ_z and θ_e . The F_2 and F_3 values of SH_3^+ are estimated by using Herschbach and Laurie's empirical relation [19]: $F_2 = 4.49 \times 10^5 \text{ dyn cm}^{-1}$ and $F_3 = -7.04 \times 10^{13} \text{ dyn cm}^{-2}$, which give $r_z(\text{SH}) - r_z(\text{SD})$ to be 0.00410 \AA . This value agrees well with 0.00426 \AA derived from the r_z structure by using the relation of the reduced mass. The determined r_e structure of SH_3^+ is listed in table 4. The present r_e structure agrees well with that predicted by the *ab initio* method [13].

References

- [1] NAKANAGA, T., and AMANO, T., 1987, *Chem. Phys. Lett.*, **134**, 195.
- [2] NAKANAGA, T., and AMANO, T., 1989, *J. molec. Spectrosc.*, **133**, 201.
- [3] AMANO, T., KAWAGUCHI, K., and HIROTA, E., 1987, *J. molec. Spectrosc.*, **126**, 177.
- [4] SAITO, S., YAMAMOTO, S., and AMANO, T., 1987, *Astrophys. J.*, **314**, L27.
- [5] LEE, S. K., OZEKI, H., SAITO, S., and YAMAMOTO, S., 1994, *Chem. Phys. Lett.*, **224**, 21.
- [6] YAMABE, T., AOYAGI, T., NAGATA, S., SAKAI, H., and FUKUI, K., 1974, *Chem. Phys. Lett.*, **28**, 182.
- [7] KARI, R. E., and CSIZMADIA, I. G., 1975, *Can. J. Chem.*, **53**, 3747.
- [8] SO, S. P., 1979, *Chem. Phys. Lett.*, **61**, 83.
- [9] DIXON, D. A., and MARYNICK, D. S., 1979, *J. chem. Phys.*, **71**, 2860.
- [10] SCHMIEDEKAMP, A., CRUICKSHANK, D. W. J., SKAAARUP, S. PULEY, P., HARGITTAL, I., and BOGGS, J. E., 1979, *J. Am. Chem. Soc.*, **101**, 2002.
- [11] MARKHAM, G. D., and BOCK, C. W., 1993, *J. chem. Phys.*, **97**, 5562.
- [12] DEFREES, D. J., and MCLEAN, A. D., 1985, *J. chem. Phys.*, **82**, 333.
- [13] BOTSCHWINA, P., ZILCH, A., WERNER, H.-J., ROSMUS, P., and REINSCH, E.-A., 1986, *J. chem. Phys.*, **85**, 5107.
- [14] XIA, C., SANZ, M. M., and FOSTER, S. C., 1998, *J. molec. Spectrosc.*, **188**, 175.
- [15] HELMS, D. A., and GORDY, W., 1977, *J. molec. Spectrosc.*, **66**, 206.
- [16] OKA, T., 1960, *J. Phys. Soc. Jpn.* **15**, 2274.
- [17] CHU, F. Y., and OKA, T., 1974, *J. chem. Phys.*, **60**, 4612.
- [18] OKA, T., and MORINO, Y., 1962, *J. molec. Spectrosc.*, **8**, 300.

[19] HERSCHBACH, D. R., and LAURIE, V. W., 1961, *J. chem. Phys.*, **35**, 458.

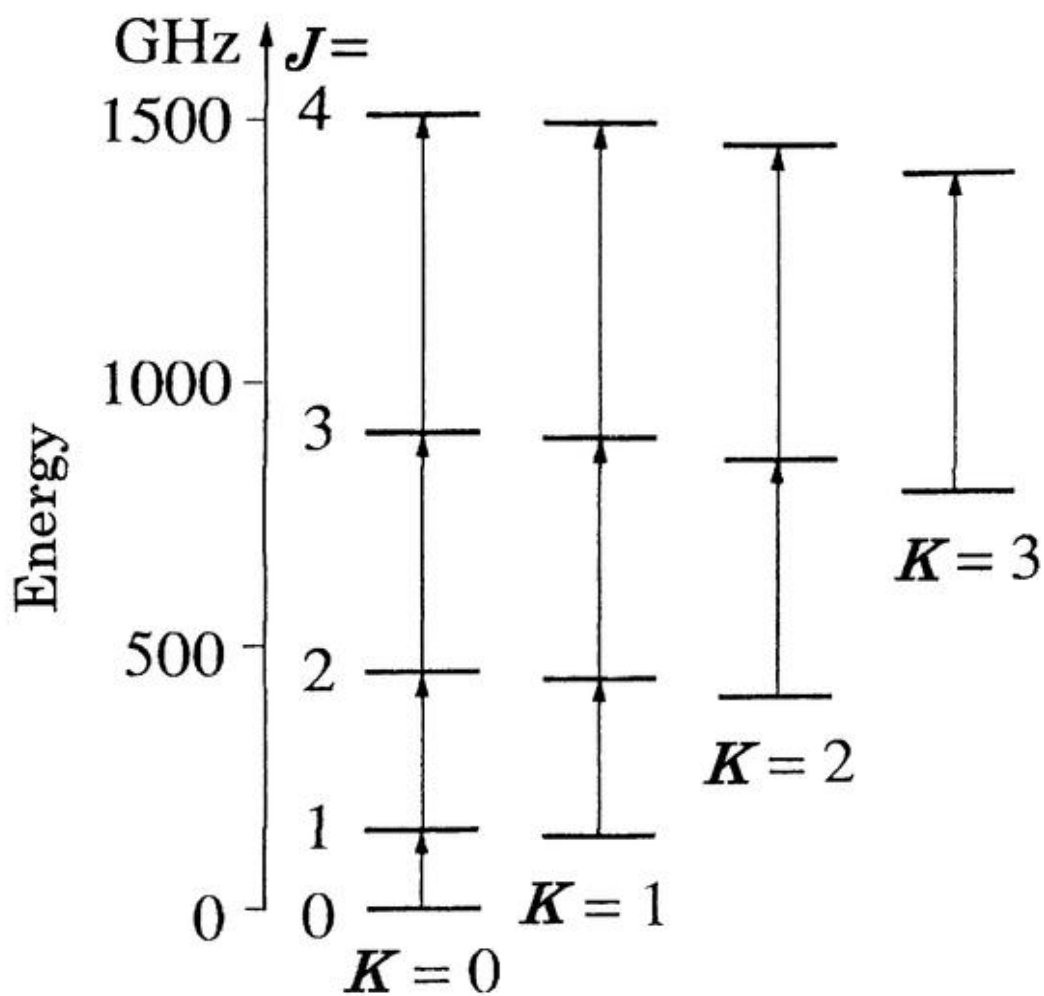


Figure 4.1. Energy diagram of SD_3^+ and the observed transitions.

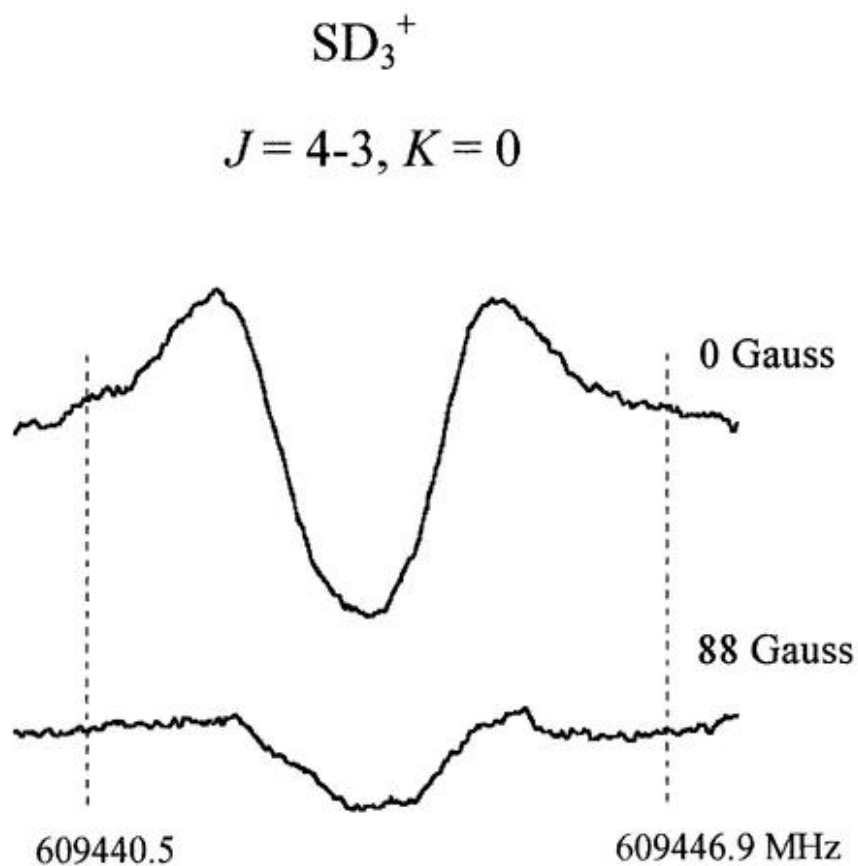


Figure 4.2. The $J = 3 - 4, K = 0$ transition of SD_3^+ observed with a hollow-cathode discharge cell. SD_3^+ was produced by DC-glow discharge of 500 mA with mixture of D_2S (5 mTorr) and D_2 (10 mTorr). The integration time was 20 s (100 scans). The upper trace was obtained without a magnetic field, whereas a field of 88 G was applied in recording the lower trace.

Table 1. Observed and calculated transition frequencies of SD_3^+ (MHz).

J'	J''	K	$\nu_{\text{obs}}^{\text{a}}$	$\nu_{\text{corr}}^{\text{b}}$	$\Delta \nu^{\text{c}}$
1	0	0	152431.301(16)	152431.290	.049
2	1	0	304834.415(6)	304834.392	.022
2	1	1	304840.684(24)	304840.616	-.001
3	2	0	457181.283(14)	457181.249	-.025
3	2	1	457190.620(12)	457190.586	-.059
3	2	2	457218.816(10)	457218.782	.025
4	3	0	609443.897(23)	609443.852	.011
4	3	1	609456.419(17)	609456.374	.039
4	3	2	609493.826(10)	609493.781	-.037
4	3	3	609556.344(17)	609556.299	.009

^a Values in parentheses denote one standard deviation of the frequency measurement and apply to the last digits of the frequencies.

^b Corrected frequencies for the ion-drift Doppler shift. These values were used in the least squares fitting.

^c Residuals in the least squares fit, $\Delta \nu = \nu_{\text{obs}} - \nu_{\text{calc}}$.

Table 2. Molecular constants of SD_3^+ (MHz).

Constants	This work ^a	Infrared ^{a,b}	<i>Ab initio</i> ^c
B_0	76217.9633(190)	76218.6(45)	76270
D_J	1.17135(73)	1.17(30)	1.132 ^d
D_{JK}	-1.5618(20)	-1.54(90)	-1.499 ^d

^a Values in parentheses denote three times the standard deviation and apply to the last digits of the constants.

^b Xia *et al.* (14)

^c Botschwina *et al.* (13).

^d D_J^{e} and D_{JK}^{e} .

Table 3. Zero-point corrections of SH_3^+ and SD_3^+ .

	SH_3^+	SD_3^+
B_0	146737.674(37)	76217.9633(190)
δB	-1639(49) ^a	-611.0(183) ^a
B_z	145099(49)	75606.9(183)
C_0	126760.0(32)	63619(15) ^b
δC	-1190(36) ^a	-416.1(125) ^a
C_z	125534(39)	63190(28)

^a The uncertainties in the zero-point corrections of rotational constants estimated to be 3%.^b Calculated from the estimated molecular structure, see text.Table 4. Molecular structure of SH_3^+ and SD_3^+ .^a

		Effective (r_0)	Average (r_z) ^b	Equilibrium (r_e)
SH_3^+	r (Å)	1.3578717(57)	1.36512(22)	1.35001(113)
	α (°)	94.17252(108)	94.098(26)	94.181(135)
SD_3^+	r (Å)	1.355690(45)	1.36086(16)	
	α (°)	94.187 ^c	94.1211(195)	

^a Values in parentheses are three standard deviation and apply to the last digits of the constants.^b The error of the r_z structure was caused by the uncertainties in the zero-point corrections of rotational constants. The uncertainties were estimated to be 3% of the correction.^c Fixed at an estimated value (see text). The error was assumed to be 0.01°.

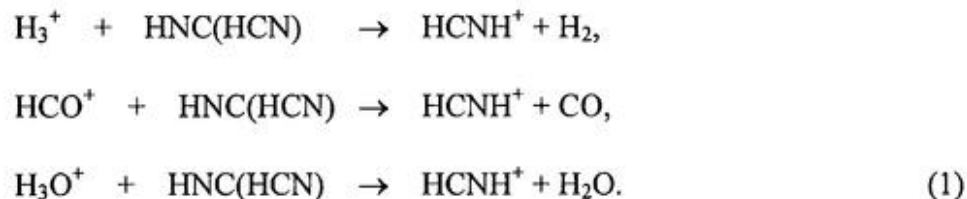
5. Microwave Spectra of the Pure Rotational Transitions of HCNH^+ and its Isotopic Species

[*The Astrophysical Journal*, **496**, L53 (1998)]

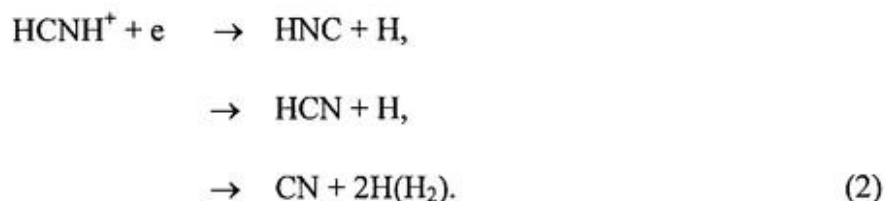
5.1 Introduction

The protonated hydrogen cyanide ion, HCNH^+ , has drawn much attention because of its importance in the chemistry of interstellar clouds. HCNH^+ was first detected toward Sgr B2, a huge molecular cloud and ionized atomic hydrogen region complex in the Galactic Center, by Ziurys and Turner [1], who observed three rotational transitions of $J = 1 - 0$ to $3 - 2$. The fractional abundance of HCNH^+ was estimated to be 3×10^{-10} . Later, Ziurys *et al.* [2] tried to observe HCNH^+ in the dark clouds and succeeded in detecting it toward TMC-1 (Taurus Molecular Cloud 1: dark cloud), with the fractional abundance estimated to be 3×10^{-9} . The hyperfine structure of the $J = 1 - 0$ transition was resolved and the quadrupole coupling constant eQq of the nitrogen nucleus was determined. Interestingly, these abundances in both types of clouds are generally higher than those predicted by several model calculations [3-6].

The main formation reactions of HCNH^+ in dark clouds are the following (e.g., [7]);



Furthermore, HCNH^+ is a precursor of HCN, HNC, and CN by dissociative recombination with electron;



HCN, HNC, and CN have been observed to be abundant in many interstellar clouds. The higher abundance of HNC than that estimated from thermodynamical equilibrium in the interstellar cloud is a convincing evidence that suggests the contribution of these reactions [7-9]. So far, the branching ratio of this reaction was predicted from a theoretical calculation by Talbi *et al.* [10] and has not been measured in a laboratory experiment. It can be said that the HCNH^+ ion is ubiquitous in molecular clouds and plays an important role in interstellar hydrogen cyanaide chemistry.

The isotopic species of HCN and HNC are the precursors or the reaction products of HCNH^+ , as seen in reactions (1) and (2), and are also known to show significant deuterium enrichment in the interstellar media [11-17]. The high abundance of the deuterium species can be mostly explained by chemical fractionation at a low-temperature environment as discussed in the Introduction. However, the observation of DCN or DNC in a hot region like Orion-KL strongly suggests an involvement of dusts in the formation or storage process, i.e., sublimation of the fossil molecule from the dusts [16]. The observation of the deuterium species of the HCNH^+ ion, HCND^+ and DCNH^+ , is essential to a thorough understanding of cyanide chemistry in the interstellar media. In that sense, laboratory spectroscopy of HCNH^+ and its isotopic species is quite important for providing the rest frequencies of the rotational transitions to astronomical search.

There are many laboratory spectroscopic reports for vibration-rotation transitions of HCNH^+ in the infrared region (e.g., [18-20]). The $J = 2 - 1$, $3 - 2$, and $5 - 4$ transitions of

HCNH^+ were observed by Bogey *et al.* [21] in the millimeter and submillimeter wave region, and the molecular constants were obtained. Based on these results, HCNH^+ was detected in interstellar clouds.

On the contrary, the microwave spectroscopic study of the deuterated species has not been done. Bogey *et al.* [21] reported a tentative detection of DCNH^+ at 370 GHz region ($J = 6 - 5$); however it has not been confirmed. For the vibration-rotation transitions of isotopic species in the infrared region, the ν_2 band of HCND^+ and the ν_1 band of $\text{H}^{13}\text{CNH}^+$ were observed by Amano and Tanaka [22], and they determined the r_s structure which is derived from isotopic effect. The ν_1 band of DCNH^+ was reported by Amano [18]. The experimental errors of the rotational transitions derived from their molecular constants are about several MHz or more, which are not accurate enough to search the molecule in astronomical observations. This chapter describes the laboratory microwave spectroscopy of the HCNH^+ ion and its deuterated species for providing accurate rest frequencies of their rotational transitions.

5.2 Experimental

Pure rotational transitions of the HCNH^+ , HCND^+ and DCND^+ were observed using the experimental apparatus described in chapter 2. The HCNH^+ was generated by the DC-glow discharge in HCN (1 mTorr) at -100 to -140°C. The DCND^+ was generated with DCN (5 mTorr), and the HCND^+ was generated with the gas mixture of HCN (2 mTorr) and DCN (5 mTorr). The method of a magnetically confined DC-glow discharge was employed for efficient production of protonated ions, which was enhanced by the lengthening of the ion-rich negative glow and the increase of ionizing electron density, as

described in chapter 2 [21,23]. The optimum magnetic field was about 130 Gauss, and the discharge current and voltage were 40 mA and 2200 V, respectively. Signal intensities of the observed lines were enhanced because of the magnetic field, confidently indicating the lines to be the transitions of protonated ions. The dependence of the $J = 6 - 5$ transition of HCND^+ on the magnetic field is shown in figure 5.1.

For the HCNH^+ ion, three lines were remeasured that were already reported by Bogey *et al.* [21], and two other lines were newly measured in the present study. On the basis of their observation toward TMC-1, Ziurys *et al.* [2] determined the eQq constant of the nitrogen nucleus to be -0.49 MHz. For the observed $J = 2 - 1$ line in the present study, the hyperfine splitting by the eQq interaction of the nitrogen nucleus was not resolved. The full width at half maximum of the $J = 2 - 1$ transition was about 400 kHz, which is mainly due to pressure broadening and is not narrow enough to resolve the hyperfine structure. The frequencies of DCND^+ were predicted from the r_s structure [22]. For HCND^+ , the frequencies have been predicted from the molecular constants determined by the infrared study [22]. The lines of the HCND^+ and DCND^+ were detected within estimated error ranges. The frequencies of DCNH^+ were also predicted from the molecular constants obtained from infrared spectra [18]. Several attempts were made to detect DCNH^+ , but they were unsuccessful because of the small dipole moment, as discussed later. All the observed line frequencies of three isotopic species are listed in table 1, and the transitions are described in energy diagram as shown in figure 5.2.

The observed frequency may include an ion-drift Doppler shift, and we measured difference between the observed frequencies of the $J = 5 - 4$ transition of HCNH^+ in normal and opposite electrode configurations, where in the normal one, microwave

radiation propagated from the anode to the cathode, and in the opposite one, the propagation was reversed. However, corrections due to the drift Doppler shift turned out to be unnecessary for all the measured lines because the amount of shift was smaller than our experimental accuracy of several tens of kilohertz (table 1).

5.3 Rest frequencies for astronomical searches

The observed line frequencies of HCNH^+ , HCND^+ and DCND^+ were analyzed using a rotational energy formula of a linear molecule with a least-squares method. The molecular constant for each species was precisely determined. Two transitions of HCNH^+ were newly measured, in addition to those measured in a previous study [21]; consequently, the precision of the determined rotational and centrifugal distortion constants was improved by about one order of magnitude. The standard deviation of HCNH^+ lines decreased by about one order of magnitude from the previous values. For HCND^+ , the accuracy of the rotational constant was improved by more than two orders of magnitude from the previous infrared study. The DCND^+ ion was spectroscopically detected for the first time. These molecular constants were calculated with the rotational energy formula for the linear molecule in the ground vibrational state and are listed in table 2. The accuracy of the rest transition frequencies is around several tens of kilohertz, and they are now available for the astronomical search. By Doppler shift due to drift of a molecular cloud, observed frequency toward the cloud is shifted from the rest frequency measured in a laboratory spectroscopy. The accurate rest frequency is essential to determine the amount of Doppler shift, which indicates physical condition of the cloud.

In contrast to the above three species, the signal of DCNH^+ was not detected in this laboratory study. Although we searched the region where Bogey *et al.* [21] reported its

detection, and also that estimated from infrared study, the signal intensity was less than our detection limit. This is due to the small electric dipole moment of the molecule. Botschwina calculated this physical quantity for four isotopic species [24]. He reported that the dipole moment of HCNH^+ , HCND^+ , and DCND^+ were -0.29, -0.54, and -0.26 D, respectively, while for DCNH^+ it was reduced to 0.004 D. Our result strongly supports his calculation; its dipole moment was estimated to be at least less than 0.1 D if the statistical partitioning of the H and D atoms was assumed in the formation reaction in the discharge cell. As a result, the astronomical search for DCNH^+ in the microwave region seems to be difficult. The dipole moment of HCND^+ is about twice as larger as that of HCNH^+ [24], so that a search for it in interstellar clouds may be advantageous.

Now we concern ourselves with the possibility of the astronomical detection of the deuterated species, HCND^+ . Deuterium enrichment is observed in many molecules, such as HCO^+ , HNC , HCN , and others. The abundance ratios of their normal species of DCO^+ , DNC , and DCN in TMC-1 are 0.013 - 0.017 [25], 0.015 [25], and 0.022 - 0.024 [26], respectively. HCNH^+ is related with HNC and HCN via reactions (1) and (2), and strong deuterium enrichment is expected for the ratio of $[\text{HCND}^+]/[\text{HCNH}^+]$. Recently, Millar *et al.* [27] and Howe and Millar [17] predicted its ratio by model calculations in TMC-1 to be $[\text{HCND}^+]/[\text{HCNH}^+] = 4.9 - 8.6 \times 10^{-2}$ and $7.1 - 10 \times 10^{-2}$ in early time (3×10^5 yr) and in steady state, respectively. We employed the highest value in the present calculation, i.e., $[\text{HCND}^+]/[\text{HCNH}^+] = 0.1$.

A column density is an useful parameter which indicates the amount of a molecular species in the cloud, and a radiation temperature is brightness of the molecule. For $J + 1 \rightarrow J$ rotational transition, a relation of the column density N_{tot} and the radiation

temperature T_R was indicated by Ziurys *et al.* [28];

$$N_{\text{tot}} = (3 k \times 10^5 T_R \Delta V_{1/2} \zeta_{\text{rot}}) / \{8 \pi^3 \mu_0^2 \nu (J+1) \exp(-\Delta E/kT_{\text{rot}})[1 - J_{\nu}(T_{\text{bg}})/J_{\nu}(T_{\text{ex}})]\} \quad (3)$$

where

- $\Delta V_{1/2}$: width of the observed line,
- ζ_{rot} : partition function of summation type,
- μ_0 : permanent dipole moment,
- ν : frequency of the $J+1 \rightarrow J$ transition,
- ΔE : energy of the $(J+1)$ th rotational level above rotational ground state,
- T_{rot} : rotational temperature of the molecule,
- T_{bg} : the 2.78 K cosmic background,
- T_{ex} : excitation temperature of the molecular cloud,
- $J_{\nu}(T) = h\nu/k[\exp(h\nu/kT) - 1]^{-1}$

The radiation temperature T_R of the $J = 1 - 0$ transition and $\Delta V_{1/2}$ for HCNH^+ toward TMC-1 ($\alpha = 4^{\text{h}}38^{\text{m}}38^{\text{s}}$; $\delta = 25^{\circ}35'45''$ (1950.0)) were reported by Ziurys *et al.* [2]: $T_R = 0.42$ K and $\Delta V_{1/2} = 0.5$ kms^{-1} , where the T_R was summed over all three hyperfine components. The column density of HCNH^+ was recalculated to be $N_{\text{tot}} = 5.6 \times 10^{13} \text{ cm}^{-2}$ using a dipole moment of 0.29 D [24] and $T_{\text{rot}} = T_{\text{ex}} = 7$ K. Column density of HCND^+ toward TMC-1 is therefore $5.6 \times 10^{12} \text{ cm}^{-2}$. For the $J = 2 - 1$ and $3 - 2$ transitions, the radiation temperatures in the optically thin and local thermal equilibrium case are calculated to be about 230 and 150 mK, respectively, with the dipole moment of 0.54 D [24]. The present calculation demonstrates a high possibility of the detection of the HCND^+ ion toward TMC-1 as far as the deuterium ratio is around the order of several percent. The observation of HCND^+ may help us to understand the HCN/HNC chemistry

in the interstellar media.

References

- [1] ZIURYS, L. M., and TURNER, B. E. 1986, *Astrophys. J.*, **302**, L31.
- [2] ZIURYS, L. M., APPONI, A. J., and YODER, J. T. 1992, *Astrophys. J.*, **397**, L123.
- [3] MILLAR, T. J., FARQUHAR, P. R. A., and WILLACY, K. 1997, *Astron. Astrophys. Suppl.*, **121**, 139.
- [4] HASEGAWA, T. I., and HERBST, E. 1993, *Mon. Not. R. astron. Soc.*, **263**, 589.
- [5] HERBST, E., and LEUNG, C. M. 1989, *Astron. Astrophys. Suppl.*, **69**, 271.
- [6] LANGER, W. D., and GRAEDEL, T. E. 1989, *Astrophys. J. Suppl.*, **69**, 241.
- [7] SCHILKE, P., WALMSLEY, C. M., MILLAR, T. J., and HENKEL, C. 1991, *Astron. Astrophys.*, **247**, 487.
- [8] SCHILKE, P., WALMSLEY, C. M., PINEAU DES FORÊTS, G., ROUEFF, E., FLOWER, D. R., and GUILLOTEAU, S. 1992, *Astron. Astrophys.*, **256**, 595.
- [9] HERBST, E. 1995, *Annu. Rev. phys. Chem.*, **46**, 27.
- [10] TALBI, D., ELLINGER, Y., and HERBST, E. 1996, *Astron. Astrophys.*, **314**, 688.
- [11] WATSON, W. D. 1976, *Rev. Mod. Phys.*, **48**, 513.
- [12] BROWN, R. D. 1977, *Nature*, **270**, 39.
- [13] GODFREY, P. D., BROWN, R. D., GUNN, H. I., BLACKMAN, G. L., and STOREY, J. W. V. 1977, *Mon. Not. R. astron. Soc.*, **180**, 83p.
- [14] PENZIAS, A. A., WANNIER, P. G., WILSON, R. W., and LINKE, R. A. 1977, *Astrophys. J.*, **211**, 108.
- [15] TURNER, B. E. and ZUCKERMAN, B. 1978, *Astrophys. J.*, 225, L75.
- [16] MANGUM, J. G., PLAMBECK, R. L., and WOOTTEN, A. 1991, *Astrophys. J.*, **369**, 169.
- [17] HOWE, D. A., and MILLAR, T. J. 1993, *Mon. Not. R. astron. Soc.*, **262**, 868.

- [18] AMANO, T. 1984, *J. chem. Phys.*, **81**, 3350.
- [19] KAJITA, M., KAWAGUCHI, K., and HIROTA, E. 1988, *J. molec. Spectrosc.*, **127**, 275.
- [20] LIU, D.-J., LEE, S.-T., and OKA, T. 1988, *J. molec. Spectrosc.*, **128**, 236.
- [21] BOGEY, M., DEMUYNCK, C., and DESTOMBES, J. L. 1985, *J. chem. Phys.*, **83**, 3703.
- [22] AMANO, T., and TANAKA, K. 1986, *J. molec. Spectrosc.*, **116**, 112.
- [23] DE LUCIA, F. C., HERBST, E., PLUMMER, G. M., and BLAKE, G. A. 1983, *J. chem. Phys.*, **78**, 2312.
- [24] BOTSCHWINA, P. 1986, *Chem. Phys. Letters*, **124**, 382
- [25] GUÉLIN, M., LANGER, W. D., and WILSON, R. W. 1982, *Astron. Astrophys.*, **107**, 107
- [26] WOOTTEN, A. 1987, in *Astrochemistry*, ed. M. S. VARDYA and S. P. TARAFDAR (Dordrecht : Reidel), p. 311.
- [27] MILLAR, T. J., BENNETT, A., and HERBST, E. 1989, *Astrophys. J.*, **340**, 906.
- [28] ZIURYS, L. M., FRIBERG, P., and IRVINE, W. M. 1989, *Astrophys. J.*, **343**, 201.

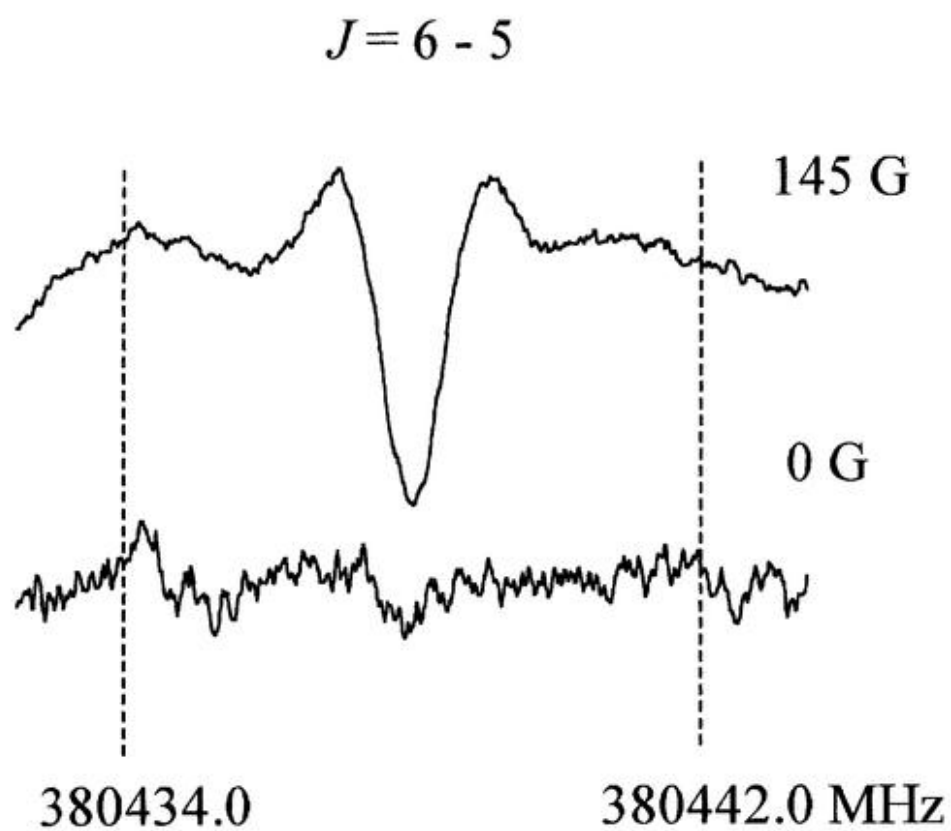


Figure 5.1. The $J = 6 - 5$ transition of HCND^+ observed in the magnetically confined DC-glow discharge where the magnetic field of 145 G in the upper spectrum and 0 G in the lower one. The spectra were obtained by 40 s averaging with a time constant of 1 ms.

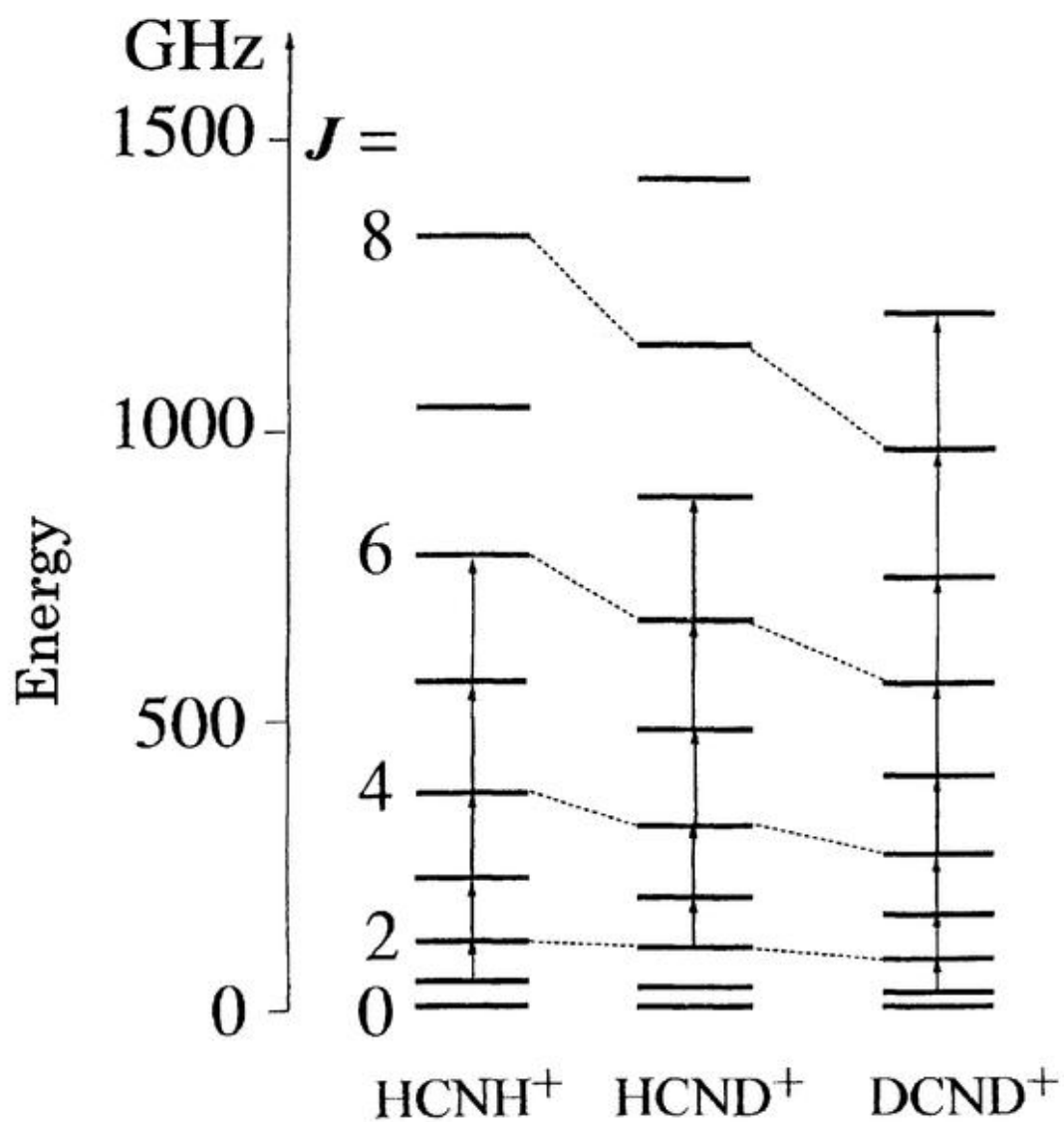


Figure 5.2. Energy diagram of HCNH^+ and its isotopic species, and the observed rotational transitions.

Table 1. Observed rotational transitions of HCNH^+ and its isotopic species (MHz).

$J''-J'$	HCNH^+		HCND^+		DCND^+	
	$\nu_{\text{obs}}^{\text{a}}$	$\Delta\nu^{\text{b}}$	$\nu_{\text{obs}}^{\text{a}}$	$\Delta\nu^{\text{b}}$	$\nu_{\text{obs}}^{\text{a}}$	$\Delta\nu^{\text{b}}$
2-1	148221.450(17)	-0.004	126821.726		107095.712(35)	-0.010
3-2	222329.310(6)	0.020	190230.470(23)	-0.012	160642.079(75)	-0.01
4-3	296433.652(17)	-0.003	253636.742(34)	0.032	214186.618(17)	-0.047 ^d
5-4	370533.375(23)	-0.020	317039.543(23)	-0.025	267728.913(18)	0.062 ^d
6-5	444627.361(10)	0.010	380438.217(28)	0.004	321268.058(10)	0.008
7-6			443831.804(17)	0.002	374803.689(7)	0.022
8-7					428335.077(25)	-0.024
9-8					481861.762(37)	0.005

^a Measurement error (σ) is given in the parentheses.^b $\Delta\nu = \nu_{\text{obs}} - \nu_{\text{calc.}}$ ^c Calculated value. The molecular constants given in table 2 are used.^d Not included in the least-squares fit.Table 2. Molecular constants of HCNH^+ and its isotopic species (MHz).^a

Constants	HCNH^+	HCND^+	DCND^+
B_0	37055.7491(74)	31705.7123(88)	26774.1295(56)
D_0	0.048193(136)	0.035109(119)	0.024888(44)
rms (kHz)	17.8	24.6	18.5

^a MHz (3σ).

6. Summary

The author examined two efficient production techniques of gaseous molecular ions; a hollow cathode discharge and a magnetically confined DC-glow discharge, and studied four kinds of deuterated molecular ions, which are important in the laboratory and astronomical spectroscopy, with millimeter- and submillimeter-wave spectroscopy.

Spectroscopic studies of the fully deuterated hydronium ion, D_3O^+ , were extremely limited, and there was no spectroscopic information of a ground state inversion splitting. Notwithstanding we observed the ground state inversion-rotation transitions of D_3O^+ for the first time by microwave spectroscopy. Fifty three P- and Q-branch transitions were measured precisely for the lowest pair levels of inversion motion in the frequency region of 220 to 565 GHz. An inclusion of the $\Delta k = \pm 3n$ interactions in the Hamiltonian was essential for a full explanation of the observed lines within measurement errors. Molecular constants for the upper (0^+) and lower (0^-) levels in the inversion motion as well as the $\Delta k = \pm 3n$ interaction parameters were obtained by a least-squares fitting to the observed spectral lines, and the rotational constants C in the 0^+ and 0^- levels were also derived by a combination of the interaction parameters and the molecular constants. The inversion splitting was accurately determined to be $15.35550086(147) \text{ cm}^{-1}$, where the number in parentheses denotes one standard deviation of the fit. Since a harmonic potential of H_3O^+ is available, zero-point corrections to the rotational constants of H_3O^+ and D_3O^+ were calculated and the zero-point averaged (r_z) structures were derived from their zero-point corrected rotational structures. From the shift between the r_z structures of H_3O^+ and D_3O^+ the r_e structure of H_3O^+ was estimated to be $r_e = 0.9780(59) \text{ \AA}$, $\theta_e = 112.8(25)^\circ$.

The $J = 1 - 0$ to $4 - 3$ spectral lines of SD_3^+ were measured in the 152 - 610 GHz

region. The rotational constant B_0 and the centrifugal distortion constants D_J and D_{JK} were determined from the measured frequencies. A vibration-rotation analysis was carried out and the r_z structures of SH_3^+ and SD_3^+ were derived from their zero-point averaged rotational constants. From the shift between the r_z structures of SH_3^+ and SD_3^+ the r_e structure of SH_3^+ was estimated to be

$$r_e = 1.35001(113)\text{\AA}, \theta_e = 94.181(135)^\circ,$$

where the number in parentheses denotes three standard deviation of the fit.

The pure rotational transitions of the protonated hydrogen cyanide ion, HCNH^+ , and its isotopic species, HCND^+ and DCND^+ , were measured in the 107 - 482 GHz region. The ions were generated in the cell with a magnetically confined DC-glow discharge of HCN and/or DCN. The rotational constant B_0 and the centrifugal distortion constant D_0 for each ion were precisely determined by the fit. The observed rotational transition frequencies by laboratory spectroscopy and the predicted ones are accurate enough to use as rest frequencies for astronomical searches of HCNH^+ and HCND^+ . The observation of the molecules in interstellar clouds will be contribute to a thorough understanding of cyanide chemistry in the interstellar media.